Visual pathways of the secondary eyes in the brain of a jumping spider

Running title: **Jumping spider secondary eye visual pathways**

Philip O.M. Steinhoff[1*], Gabriele Uhl[1], Steffen Harzsch[2] & Andy Sombke[3]

[1] Zoological Institute and Museum, General and Systematic Zoology, University of Greifswald, Loitzer Straße 26, 17489 Greifswald, Germany.

[2] Zoological Institute and Museum, Cytology and Evolutionary Biology, University of Greifswald, Soldmannstraße 23, 17489 Greifswald, Germany

[3] Department of Integrative Zoology, University of Vienna, Althanstraße 14, 1090 Vienna, Austria

[*]*Corresponding Author. E-Mail: philipsteinhoff@gmail.com*

ACKNOWLEDGEMENTS

The authors thank Matthes Kenning and Georg Brenneis (University of Greifswald) as well as Nicholas J. Strausfeld (University of Arizona, Tucson) for helpful discussions. We thank Kerstin Stejskal and Thomas Hummel (University of Vienna) for the provision of *Cupiennius salei* and Elvira Lutjanov, Christian Müller, Sabine Ziesemer and Jan-Peter Hildebrandt (all University of Greifswald) for help with western blot analysis. Monica M. Sheffer provided helpful comments that improved the manuscript. This study was financially supported by the German Research Foundation DFG UH 87/11-1 and DFG INST 292/119-1 FUGG, DFG INST 292/120-1 FUGG. POMS was additionally supported by a Bogislaw scholarship from the University of Greifswald and a Laudier Histology cooperation & travel grant.

Abstract

Some animals have evolved task differentiation of individual structures within the same sensory modality (e.g. olfaction or vision). A particular example is spiders, where most species have eight

eyes, of which two (the principle eyes) are used for object discrimination, whereas the other three pairs (secondary eyes) detect movement. In the model spider species *Cupiennius salei* (Keyserling, 1877) these two eye types correspond to two distinct visual pathways in the brain. Each eye is associated with its own first and second order visual neuropil. The second order neuropils of the principle eyes are connected to the arcuate body, whereas the second order neuropils of the secondary eyes are linked to the mushroom body. However, the secondary eye size and visual fields of *C. salei* differs considerably from that of the likewise visually hunting jumping spiders. We explored the secondary eye visual pathway of the jumping spider *Marpissa muscosa*, and found that the connectivity of neuropils differs from that in *C. salei.* In *M. muscosa,* all secondary eyes are connected to their own first order visual neuropils. The first order visual neuropils of the anterior lateral and posterior lateral eyes are further connected with two second order visual neuropils, the array of microglomeruli and the 2nd order visual neuropil of the lateral eyes, whereas the posterior median eyes lack associated second order neuropils and axons project only to the arcuate body. These differences between *C. salei* and *M. muscosa* suggest substantial differences in information processing and function of their visual neuropils.

Keywords

Secondary eyes, visual pathway, jumping spider, visual neuropils, brain, microglomeruli

1 Introduction

In some animal species with multiple eyes, different eyes serve different specific tasks. Spiders vary strongly in their visual abilities, as well as in number, arrangement and size of their eyes (reviewed in Morehouse et al. 2017). Most species possess four pairs of eyes, of which one pair differs from the three other pairs in its anatomy and developmental origin (Land, 1985b; Morehouse et al., 2017). The principle eyes (or anterior median eyes) possess a movable retina and their spectral sensitivities allow for color vision (Barth et al. 1993; Land, 1985b; A Schmid, 1998; Yamashita & Tateda, 1976, 1978). The other three pairs of eyes are the so-called secondary eyes (posterior median, anterior lateral and posterior lateral eyes). Their morphology and anatomy differs considerably among spider families (Homann, 1950, 1952), but they generally do

not have a movable retina. In several groups of cursorial hunting spiders, the secondary eyes are used for movement detection (Land, 1985b; Morehouse et al., 2017; Schmid, 1998). Most secondary eyes possess a light-reflecting tapetum (but absent in e.g. jumping spiders), which led to the assumption that they play a major role for night or dim light vision (Foelix, 1996).

Jumping spiders (Salticidae) are cursorial hunters with excellent vision. Their eyes have been studied in much greater detail compared to any other spider group (Harland, Li, & Jackson, 2012; Land, 1985b; Morehouse et al., 2017). The principle eyes of jumping spiders are large and face forward; their field of view is small, but their spatial acuity is one of the highest among invertebrate eyes (Harland et al., 2012; Land, 1985a, 1985b). The secondary eyes of salticids possess only one photoreceptor type and thus cannot discriminate colors (Yamashita & Tateda, 1976). Among the secondary eyes, the anterior lateral eyes (ALE) and posterior lateral eyes (PLE) are large, able to detect motion and elicit an orienting response of the principle eyes towards the moving object (Duelli, 1978; Jakob et al., 2018; Spano, Long, & Jakob, 2012; Zurek & Nelson, 2012a, 2012b; Zurek, Taylor, Evans, & Nelson, 2010). The posterior median eyes (PME) of most salticids (except for the non-salticoids) are very small and positioned between ALE and PLE (Land, 1985a; Maddison & Hedin, 2003). Since the fields of view of ALE and PLE overlap, the PME do not have an exclusive field of view (Land, 1985a).

While the eyes of jumping spiders have been studied in detail, less is known about the associated brain structures that process visual information (Duelli, 1980; but see Hanström, 1921; Hill, 1975; Nagata, Arikawa, & Kinoshita, 2019; Steinhoff et al., 2017). Our knowledge on the visual processing pathways in the brain of spiders is mostly based on investigations of the spider model species *Cupiennius salei* (Keyserling, 1877) (Babu & Barth, 1984; Becherer & Schmid, 1999; Schmid & Duncker, 1993; Strausfeld & Barth, 1993; Strausfeld, Weltzien, & Barth, 1993). *C. salei* possesses two separate visual pathways, one for the principle eyes and one for all secondary eyes (Strausfeld & Barth, 1993; Strausfeld et al., 1993). In *C. salei*, every eye is connected to its own first and second order visual neuropil (Barth, 2002). While the second order visual neuropils of the principle eyes are connected to the arcuate body (Strausfeld et al., 1993), the second order visual neuropils of the secondary eyes are associated to the mushroom bodies (Strausfeld &

Barth, 1993). Furthermore, the first order visual neuropils of the secondary eyes are directly connected to the arcuate body (Babu & Barth, 1984).

In *C. salei,* similar to salticids, the principle eyes are used for object recognition, while the secondary eyes serve the purpose of movement detection (Fenk, Hoinkes, & Schmid, 2010; Schmid, 1998). The secondary eyes of *C. salei* have a high spectral sensitivity, similar to the principle eyes (Barth et al., 1993). However, they are unable to detect color in moving objects (Orlando & Schmid, 2011) and similar to jumping spiders are capable of acute motion detection (Fenk & Schmid, 2010; Zurek & Nelson, 2012b). Despite these similarities in functional role and visual ability of the secondary eyes, the relative size of different eyes and thus fields of view differ considerably (Land, 1985a; Land & Barth, 1992). Furthermore, Steinhoff et al. (2017) showed that the structure and arrangement of the secondary eye visual neuropils in in the jumping spider *Marpissa muscosa* (Clerck, 1757) differ from those in *C. salei.* We thus hypothesize, that the secondary eye visual pathways of jumping spiders also differ from that in the model species *C. salei.* Here, we describe the secondary eye visual pathways in the brain of the jumping spider *M. muscosa*. We use paraffin histology, immunohistochemistry, and microCT analysis to visualize neurite tracts in the visual system. We compare our findings in *M. muscosa* with results of earlier studies and new immunohistochemical data on the secondary eye pathways in the brain of *C. salei*. We discuss the differences in their secondary eye pathways in the light of different functional roles of their eyes.

2 Material and Methods

2.1 Animals

Adult female *Marpissa muscosa* were collected in and near Greifswald (Germany). Spiders were fed on *Drosophila sp.* weekly and kept individually in plastic boxes of 145 x 110 x 68 mm size that were enriched with paper tissue.

2.2 Paraffin-histology

115 The prosomata of two females of *M. muscosa* were fixed in Dubosq–Brazil solution (1 g saturated
116 alcoholic picric acid, 150 ml 80% ethanol, 15 ml pure acetic acid, and 60 ml 37% formaldehyde).
117 After four days in fixative, the prosomata were dehydrated through a graded ethanol series (80%,
118 90%, and 3x 96% ethanol for 20 minutes each) and were then transferred for two hours into a
119 1:1 solution of 96% ethanol:tetrahydrofuran (Carl Roth, CP82.1) at room temperature. Samples
120 were kept for 24 hours in pure tetrahydrofuran followed by 24 hours in a solution of 1:1
121 tetrahydrofuran and paraffin (Carl Roth, 6643.1) at 60°C. Afterwards, samples were transferred
122 to 100% paraffin at 60°C for 48 hours and then embedded in fresh paraffin. Sagittal and
123 transversal sections (5 µm) were cut with a motorized rotary microtome (Microm HM 360).
124 Sections were stained with Azan according to Geidies (Schulze & Graupner, 1960), and mounted
125 in Roti-Histokitt II (Carl Roth, T160.1).
126
127 **2.3 MicroCT analysis**
128 Prosomata of two individuals of *M. muscosa* and one individual of *C. salei* were fixed in Dubosq–
129 Brazil solution. Prior to fixation, legs and opisthosomata were cut off and cuticle and musculature
130 were removed from the dorsocaudal part of the prosomata to allow faster penetration of the
131 fixative. After four days in fixative, samples were washed six times for 20 minutes in 0.1 M
132 phosphate buffered saline (PBS, pH 7.4) followed by dehydration in a graded ethanol series (80%,
133 90%, 96% and 3x 99,8% ethanol for 20 minutes each). Samples were then transferred to an 1%
134 iodine solution (iodine, resublimated [Carl Roth, X864.1] in 99.8% ethanol) over 48 h to enhance
135 tissue contrast (Sombke, Lipke, Michalik, Uhl, & Harzsch, 2015) and subsequently critical point
136 dried with an automated dryer (Leica EM CPD300). The protocol applied was: slow CO_2
137 admittance with a delay of 120 seconds, 30 exchange cycles, followed by a slow heating process
138 and slow gas discharge. Dried prosomata were mounted using a conventional glue gun onto
139 aluminum rods, so that the anterior median eyes were oriented upwards.
140 MicroCT scans were performed using a Zeiss XradiaXCT-200 (Sombke et al., 2015). Scans were
141 performed with a macro-, a 4x- and a 20x objective lens unit and the following settings: 40 kV
142 and 8 W or 30 kV and 6 W, 200 µA, exposure times between 2 and 4 s. Tomographic projections
143 were reconstructed with the XMReconstructor software (Zeiss), resulting in image stacks (TIFF

144 format). Scans were performed using Binning 2 for noise reduction and were reconstructed with
145 full resolution (using Binning 1).
146
147 **2.4 Immunohistochemistry**
148 Four different combinations of markers were used to visualize neuropils and connecting neurites
149 in the visual system (see Table 1 for a list of marker combinations used, and Table 2 for
150 specifications of labeling reagents).
151 After anaesthetization with CO_2, brains of 25 females of *M. muscosa* (details Tab. 2) and one
152 female of *C. salei* were dissected in PBS and fixed in 4% PFA over night at room temperature.
153 Brains were washed six times for 15 minutes each in PBS and subsequently immersed in Poly-L-
154 Lysin (Sigma-Aldrich, P4707) for one minute. Samples were then embedded in 4% agarose
155 (Sigma-Aldrich, A9414) and sectioned (80µm) with a Microm HM 650 V vibratome. After
156 permeabilization in PBS-TX (PBS, 0.3% Triton X-100 [Sigma-Aldrich, X100], 1 % bovine serum
157 albumin [Sigma-Aldrich, A2153], 0.05% Na-acide; occasionally adding 1% DMSO) for 1 h at room
158 temperature, incubation in primary antibodies took place over night at 4°C or room temperature.
159 Sections were washed in several changes of PBS-TX after the incubation. Incubation in secondary
160 antibodies or counterstains took place overnight at 4°C or room temperature. After washing in
161 several changes of PBS, sections were mounted in Mowiol (Merck 475904).
162
163 The brains of five additional females were processed as whole-mounts, using an adjusted
164 protocol after Ott (2008) (see also Steinhoff et al., 2017). Brains were dissected in TRIS buffer (0.1
165 M, pH 7.4 [Carl Roth, 4855]), and fixed in zinc-formaldehyde at room temperature under soft
166 agitation for several days. Afterwards, brains were washed in TRIS buffer three times for 15
167 minutes each and incubated in a 4:1 mixture of methanol and DMSO (Dimethylsulfoxide [Carl
168 Roth, 4720]) for 2 h. After incubation in 100% methanol for 1 h, brains were rehydrated in a
169 graded series of methanol (90%, 70%, 50%, 30%) for 10 minutes each and washed in TRIS buffer.
170 This was followed by permeabilization in PBS-DMSO (PBS, 5% bovine serum albumin, 1% DMSO,
171 0.05% Na-acide) for 2 h at room temperature and incubation in primary antibody for 4 days at
172 4°C. Brains were then washed several times for 2 h in PBS-DMSO and incubated in secondary

173 antibody for 4 days at 4°C, and transferred to a graded series of glycerol, with 1%, 2%, 4% (for
174 two hours each) and 8%, 15%, 30%, 50%, 60%, 70%, 80% (for one hour each) glycerol in TRIS
175 buffer and 1% DMSO. After five changes in pure ethanol for 30 minutes each, brains were
176 mounted in fresh methyl salicylate (Sigma, 76631). In control experiments, in which we replaced
177 the primary antibodies with PBS-TX, no neuronal labeling was detected.
178
179 **2.5 Western Blot**
180 In western blots of *Drosophila melanogaster* Meigen, 1830 head homogenates (Klagges et al.,
181 1996), the monoclonal antibody mouse anti-*Drosophila* synapsin ‘‘Synorf 1‘‘ (provided by E.
182 Buchner, Universität Würzburg, Germany; raised against a *Drosophila* Glutathione S-
183 Transferase(GST)-synapsin fusion protein) recognizes at least 4 synapsin isoforms (ca. 70, 74, 80,
184 and 143 kDa). In western blot analyses in Crustacea (Harzsch & Hansson, 2008; Sullivan, Benton,
185 Sandeman, & Beltz, 2007) and Chilopoda (Sombke, Harzsch, & Hansson, 2011), isoforms in the
186 same range were recognized. Furthermore, the Synorf 1 antibody labels synaptic neuropil in taxa
187 as diverse as Araneae (Nagata et al., 2019; Steinhoff et al., 2017), Chaetognatha (Harzsch &
188 Müller, 2007) and Plathelminthes (Cebrià, 2008), suggesting that the epitope that this antiserum
189 recognizes is highly conserved. To test this, we conducted a western blot analysis as well, in which
190 we compared brain tissue of *D. melanogaster* and *M. muscosa*. The antibody provided similar
191 results for both species, staining 1 strong band at ca. 70 kDa, and in *M. muscosa* another weak
192 band around 60 kDa. This result suggests that the epitope that Synorf 1 recognizes is conserved
193 between *D. melanogaster* and *M. muscosa*.
194
195 **2.6 Microscopy, image processing and nomenclature**
196 Immunohistochemically labelled sections and whole-mounts were examined and photographed
197 with a Leica SP5 II confocal microscope (cLSM). Paraffin sections were examined and
198 photographed with a Nikon eclipse 90i microscope. 3D-visualization of microCT image stacks was
199 prepared in AMIRA 6.0.0 (ThermoFisher). An interactive 3D-visualization of the microCT
200 reconstructions was created using ImageJ 1.51n and Adobe Acrobat Pro 9.0 (see supporting
201 information; Figure S1). Images were processed in Corel PaintShop Pro using global contrast and

brightness adjustment features as well as black and white inversion. Schematic drawings were generated using Corel Draw 20.1 and figure plates were assembled in Corel PaintShop Pro 21.0. A color code for all depicted structures, as used in Loesel et al. (2013) and Steinhoff et al. (2017), was used for 3D visualizations and the schematic drawings. The terminology used for brain structures follows Richter et al. (2010). For structures specific to spiders, we use terms according to Lehmann et al. (2016). Positional information is given with respect to the body axis.

Abbreviations

AB	Arcuate body
ALE	Anterior lateral eyes
AL1	First order visual neuropils of ALE
AL1x	Neuropilar subunit of the AL1
AME	Anterior median eyes
AM1	First order visual neuropils of AME
AM2	Second order visual neuropils of AME
L2	Second order visual neuropils of anterior and posterior lateral eyes
MB	Mushroom bodies
MBbr	Mushroom body bridge
MBn	Neurites between pedunculus and microglomeruli
MG	Array of microglomeruli (second order visual neuropils of ALE and PLE in *M. muscosa*)
MBh	Mushroom body haft
MBp	Pedunculus of the mushroom body
MBs	Mushroom body shaft
PLE	Posterior lateral eyes
PL1	First order visual neuropils of the PLE
PL1x	Neuropilar subunit of the PL1
PME	Posterior median eyes
PM1	First order visual neuropils of the PME
PM2	Second order visual neuropils of the PME
SC1-3	Protocerebral soma cluster 1-3

3 Results

3.1 General organization of the protocerebrum

In *Marpissa muscosa,* the protocerebrum comprises bilaterally paired neuropils of the visual system and the mushroom body as well as the unpaired arcuate body (Fig. 1; for details see Steinhoff et al., 2017). All neuropils of the visual system are recognizable in paraffin sections (Figs. 2, 3) and microCT analysis (Fig. 4; supporting information, Fig. S1), and are characterized by a

240 strong synapsin-immunoreactivity (Figs. 5A-D; 6A, B). Tracts and individual neurites exhibit
241 prominent tubulin-immunoreactivity (Figs. 1, 5, 6). Furthermore, the optic nerves (between
242 retinae and first order visual neuropils) and the corresponding first order visual neuropils are
243 recognizable by anti-histamine labeling that also distinctly visualizes termination sites of retinula
244 cell axons (Fig. 7). A soma cortex including three discernable protocerebral clusters (Figs. 1; 2B-
245 D; 3; 5A-B, D; 6A–D) surrounds most of the synganglion. Soma cluster 1 (SC1) is located between
246 the first order visual neuropils of the lateral eyes and the array of microglomeruli (MG), cluster 2
247 (SC2) medially to the MG, and cluster 3 (SC3) anteromedially to the mushroom body bridge
248 (MBbr) (Fig. 1).
249
250 **3.2 Connectivity of the first order visual neuropils of the anterior and posterior lateral eyes**
251 The retinae of the anterior lateral eyes (ALE) and posterior lateral eyes (PLE) are connected with
252 their respective first order visual neuropils (AL1 and PL1) *via* short, thick optic nerves (Figs. 3, 5A,
253 C). A subpopulation of histaminergic retinula cell axons terminates in distinct distal layers of these
254 neuropils (AL1x and PL1x; Fig. 7A–C). Both the AL1 and PL1 are connected to the second order
255 visual neuropil of the lateral eyes (L2) and the MG via prominent tracts of parallel ordered
256 neurites that exhibit strong tubulin-immunoreactivity (Figs. 1; 5A-B, D; 6A-B). This connectivity is
257 also evident in both histological sections (Fig. 2) and microCT analysis (Fig. 4). The tracts are
258 predominantly formed by neurites that originate in the SC1, which surrounds this region of the
259 anterior protocerebrum laterally, dorsally and medially (Figs. 1; 2B-D; 5A-B; 6B, D). The L2 and
260 the MG are bi-lobed, which corresponds to the separate inputs from AL1 and PL1 (Figs. 4B, D; 5A;
261 6A, C; 8A, B). In histological sections, a thin but conspicuous tract is detectable that passes
262 between L2 and MG and likely terminates in the arcuate body (AB) (Figs. 3A, C; 6B). The neurites
263 forming this tract might originate in the SC1 and further innervate the AL1 and PL1, as well as the
264 PM1 (see below; Figs. 3; 5D).
265
266 **3.3 Connectivity of the first order visual neuropils of the posterior median eyes**
267 The posterior median eyes (PME) are much smaller than all three other pairs of secondary eyes,
268 and so is their retina (Fig. 4C, E). Because of the small retina, only a thin but long nerve, which

enters the protocerebrum between the AL1 and PL1, connects the PME to its first order visual neuropil (PM1) (Figs. 2A; 4E; 5C, C'; 10A). The PM1 is situated between AL1 and PL1 (Figs. 2A-B; 3A-B, 4E, F; 5C-D; 6B; 7A). A prominent tract projects from the PM1 to the dorsoventral part of the protocerebrum and seems to terminate in the anterolateral apices of the AB (Fig. 3A-B).

3.4 The array of microglomeruli and the mushroom body

The array of microglomeruli (MG) is divided into two lobes that tightly adjoin dorsally and are fused in the ventral part (Figs. 2C-D; 6A, C, D; 8A-B). Thus, only a uniform array is visible in most sections (e.g. Figs. 3B; 4E; 5B-C, D). Each microglomerulus is composed of a high number of synaptic complexes (Fig. 8C–E). These synaptic complexes can be visualized by anti-synapsin labeling and phalloidin-labeling (Fig. 8D, E). Individual microglomeruli are innervated by neurites originating in the AL1 and PL1 (Figs. 5A, B, D; 6D). Anti-tubulin labeling reveals that neurites interweave the microglomeruli mostly in parallel from proximal to distal (Fig. 5A). Within the core-region of the array, tubulin-immunoreactive neurites are more abundant (Fig. 5B). Two neurite bundles (MBn) connect the MG and the mushroom body pedunculus (MBp) and form a distinct chiasm close to the array (Figs. 6A, C-D; 8A-B). Neurites from the medial SC2 contribute to these bundles by projecting into the MG and into the MBp (Figs. 1; 5A-C; 6A, D). Other neurites from SC2 pass between MG and MBp towards the L2 (Fig. 5B, D). Thus, a large number of interweaving neurites characterizes the region of the MBn, which makes tracing of individual trajectories difficult (Fig. 6A–D).

Some long neurites that appear to originate in SC2 project along the periphery of the MBp and join with neurites arising from the mushroom body haft (MBh). Together they form the mushroom body bridge (MBbr) (Figs. 1; 5C; 6A, C-D). Other peripheral neurites from SC2 enter the MBh, where they seem to terminate (Figs. 1; 4B, D, F; 6D)

4 Discussion

The few comparative neuroanatomical studies on different species show that general brain anatomy varies considerably in spiders (Hanström, 1921; Hill, 1975; Long, 2016; Steinhoff et al., 2017; Weltzien & Barth, 1991). A previous investigation on the general brain anatomy of

298 *Marpissa muscosa* (Steinhoff et al., 2017) suggested that the brains of jumping spiders and the
299 model spider species *Cupiennius salei* differ in more than structure and arrangement of neuropils.
300 Indeed, we have shown here that the connectivity of neuropils in the secondary eye pathways
301 differs greatly between these two species, which suggests principle differences in the information
302 processing and function of visual neuropils.
303 The relative size and position of the secondary eyes differs between *M. muscosa* and *C. salei.*
304 While in *M. muscosa* the PME is very small and oriented sideways, it is the largest eye in *C. salei*
305 and oriented forward (Fig. 10). The PLE are similar in relative size and position, but the ALE are
306 considerably smaller in *C. salei,* albeit also oriented forward (Fig. 10). The relative size of the
307 retinae as well as the brain is smaller in *C. salei*, which is why the optic nerves associated with
308 the PME are much longer in *C. salei* (Fig. 10).
309
310 **4.1 Connectivity of the first order visual neuropils of the anterior and posterior lateral eyes**
311 In *M. muscosa*, all retinula cell axons seem to terminate in the first order visual neuropils (Fig. 7).
312 This is similar to what has been found in other Araneae (Becherer & Schmid, 1999; Duelli, 1980;
313 Schmid & Duncker, 1993; Strausfeld & Barth, 1993; Strausfeld et al., 1993). However, this pattern
314 is different in all other investigated taxa of Chelicerata (e.g. Scorpiones, Xiphosura, or
315 Pycnogonida), where a subset of retinula cell axons also projects into the second order visual
316 neuropils (Battelle, Sombke, & Harzsch, 2016; Lehmann & Melzer, 2013, 2018). In *M. mu*scosa,
317 both AL1 and PL1 each possess a ventrally located neuropilar substructure (AL1x and PL1x), which
318 is innervated by retinula cell axons (Fig. 7). This can be clearly detected by anti-histamine labeling
319 (Fig. 7), which is known to consistently label retinula cell axons and their terminals in the visual
320 systems of arthropods (Battelle et al., 1991; Harzsch et al., 2006; Harzsch, Wildt, Battelle, &
321 Waloszek, 2005; Nässel, 1999; Schmid & Duncker, 1993; Sombke & Harzsch, 2015). In our
322 histological sections, it appears as if the neurites that form the tract between AL1, PL1 and the
323 AB, arise in AL1x and PL1x respectively (Fig. 3A, C). Indeed, Hill (1975) described that neurites
324 from the AL1x domain contribute to a tract projecting towards the posterior protocerebrum. Hill
325 (1975) did not mention terminations of retinula cell axons in the AL1x and PL1x, but detected
326 neurites connecting the AL1 with the AL1x. Thus it is possible that Hill (1975) either

327 misinterpreted retinula cell axons as interneurons, or that we missed the connecting neurites
328 between AL1 and AL1x.
329 The convoluted first order visual neuropils of the ALE and the PLE are both connected with the
330 MG and the L2, as well as with the AB (Figs. 1; 2; 3A, C; 4A–D; 5A–B; 10A). These findings are
331 consistent with Hill's (1975) study on the nervous system in *Phidippus* spp., although he only
332 found that axons of the AL1, and not the PL1, join the tract that projects towards the AB. Duelli
333 (1980) however, did not detect connections between PL1 and L2 in the salticids *Evarcha arcuta*
334 (Clerck, 1757) and *Pseudamycus validus* (Thorell, 1877). He described "large field horizontal
335 neurons," closely bypassing the MG and L2 and connecting the PL1 with the posterior
336 protocerebrum (Duelli, 1980). Judging from their structure and position, these neurons might be
337 identical with the neurites described in our study and contribute to the tract that connects the
338 first order visual neuropils of the secondary eyes with the arcuate body (Fig. 3). This discrepancy
339 might be due to incomplete staining in the earlier studies where reduced-silver staining was
340 employed. Our approach combines both specific and broader markers with specific staining
341 techniques. It should also be noted that studies on the secondary eye pathways in jumping
342 spiders were conducted on different species. However, is seems unlikely that the secondary eye
343 pathways differ considerably within salticoid jumping spiders (Maddison & Hedin, 2003).
344 Based on our results, MG and L2 are shared second order visual neuropils of both AL1 and PL1 in
345 *M. muscosa*. The situation in *C. salei* is, however, different. Here, the first order visual neuropils
346 of all three secondary eyes are connected to individual second order visual neuropils (Strausfeld
347 & Barth, 1993). Each of these second order visual neuropils is composed of small neuropilar
348 glomeruli, similar to the microglomeruli that form the MG in *M. muscosa* (Fig. 9; see below). An
349 unstructured second order visual neuropil (without microglomeruli), such as the L2, is absent in
350 *C. salei* (Strausfeld & Barth, 1993; Fig. 9A). Similar to the "giant interneurons" described for
351 jumping spiders by Duelli (1980), Strausfeld & Barth (1993) detected "lamina wide-field neurons"
352 that connect all first order visual neuropils with a region close to the AB. It is very likely that these
353 neurons correspond to the axons forming the tract between first order visual neuropils and the
354 AB that we described in *M. muscosa*.
355

356 **4.2 First order visual neuropils of the posterior median eyes**

357 The PM1 is by far the smallest first order visual neuropil of all secondary eyes in *M. muscosa*. This
358 correlates with the much smaller overall size of the PME (compared to ALE and PLE). The PME
359 have previously been considered vestigial (Land, 1972, 1985b), but since there is an optic nerve
360 and a corresponding first order visual neuropil, we conclude that these eyes are functional (Figs.
361 2A; 3A-B; 4E-F; 5C-C'; 7A-B; 10A). Previously, Steinhoff et al. (2017) considered the PM1 to be a
362 second order visual neuropil ("PM2"), based on its close spatial relationship with the AL1x
363 (previously considered as PM1 by Steinhoff et al. (2017)). However, we now demonstrate that
364 the PM1 is innervated only by retinula cell axons originating in the PME, and connections
365 between PM1 and AL1x seem to be absent. This coincides with Hill's (1975) description for
366 *Phidippus* spp., although he described additional neurites connecting PL1 and PM1. It is likely that
367 these neurites contribute to the tract that connects the first order visual neuropils with the AB
368 (compare Fig. 3), instead of actually forming synapses in the PM1. The PM1 differs from all other
369 eyes by being connected to the AB only. Consequently, the pathway of the PME lacks a second
370 order visual neuropil. Information from this eye is not processed within the mushroom bodies,
371 but exclusively in the arcuate body.

372

373 **4.3 Microglomeruli**

374 Visual neuropils with a microglomerular structure have been found in the protocerebrum of
375 several spider species (e.g. Long, 2016). They have been termed "lame glomerulee" by Saint-
376 Remy (1887) and Hill (1975), "glomeruli" by Hanström (1921) and Babu & Barth (1984),
377 "spherules" by Strausfeld & Barth (1993) and "microglomeruli" by Steinhoff et al. (2017). The
378 presence and arrangement of these microglomerular neuropils differs between spider species
379 (Hanström, 1921; Long, 2016) and some authors have considered them as a substructure of the
380 MB (Babu & Barth, 1984; Hill, 1975), whereas others have considered them to be separate second
381 order visual neuropils (Long, 2016; discussed in Steinhoff et al., 2017; Strausfeld & Barth, 1993).
382 In *M. muscosa,* the MG consist of two partially fused arrays, which are connected with the AL1
383 and PL1, respectively (Figs. 1; 2; 4A-D; 5A-B; 10). They are formed by neurites originating from
384 SC2 that synapse with neurites originating from AL1 and PL1 (Figs. 5A-B; 6A, D). Thus, the MG

385 represent two closely adjoining second order visual neuropils of the ALE and PLE, respectively. In
386 *M. muscosa*, the MG was also found to react less plastically to different environmental conditions
387 than the MBp (Steinhoff et al., 2018), which was interpreted as further evidence for their function
388 as discrete visual neuropils. Each microglomerulus consists of numerous synaptic complexes (Fig.
389 8). Duelli (1980) estimated roughly 400 synapses per microglomerulus in the jumping spider
390 *Evarcha arcuta*. In neopteran insects, synaptic complexes (consisting of one presynaptic bouton,
391 surrounded by many postsynaptic boutons) are often referred to as microglomeruli (definition in
392 Rössler, Spaethe, & Groh, 2017). Previous studies in these insects used anti-synapsin labeling to
393 detect presynaptic sites, and phalloidin (which labels f-actin) to highlight postsynaptic sites (Groh
394 & Rössler, 2011). The arrangement of synaptic complexes as conspicuous microglomerular
395 structures is, however, highly variable among neopteran insects (Groh & Rössler, 2011). To
396 investigate the MG of *M. muscosa*, we have employed the same double-labeling approach (Fig.
397 8D-E) but the anti-synapsin and phalloidin labeled areas in each synaptic complex were not
398 clearly differentiated, as is the case in social hymenopterans (Groh & Rössler, 2011), despite co-
399 localization being minimal. Instead, every microglomerulus is composed of numerous boutons
400 that are either synapsin-immunoreactive or labelled by phalloidin (Fig. 8D-E). This might indicate
401 that phalloidin does not consistently label postsynaptic sites in *M. muscosa*, or that the
402 organization of the pre- and postsynaptic sites within the MG of *M. muscosa* differ compared to
403 the mushroom body calyces of investigated insect species. To clarify synaptic connectivity within
404 the MG in *M. muscosa* and spiders in general, a detailed transmission electron microscopic study
405 is needed.
406
407 **4.4 Mushroom body pedunculus, haft and bridge**
408 The neurites that connect the second order visual neuropils to the MBp have their somata in SC2
409 (Figs. 5A; 6A, C). These somata have been referred to as "globuli cells" (Hanström, 1921; Steinhoff
410 et al., 2017) or "T-cells" before (Strausfeld & Barth, 1993). In *C. salei*, globuli cells have a smaller
411 diameter of the soma and nucleus than other cell bodies in the protocerebrum (Babu & Barth,
412 1984). We could not find such size differences in *M. muscosa*. In fact, all three nuclear markers
413 revealed that somata of the three identified clusters as well the somata of the surrounding cortex

414 exhibit a similar size (Figs. 1; 2; 3; 5; 6). Thus, it is not certain whether somata of SC2 represent
415 globuli cells. The long neurites that connect the SC2 with the MG and the L2 are probably "stem
416 neurites" (Hesse & Schreiber, 2015), from which dendrites branch into the MG and L2
417 respectively, and axons project into the MBp, MBh and MBbr. A similar arrangement has been
418 described by Babu and Barth (1984) for *C. salei* and by Hill (1975) for two *Phidippus* species.
419 The structure and organization of the MB differs between *M. muscosa* and *C. salei*, as already
420 reported by Steinhoff et al. (2017). The MBh is a separate structure of the mushroom body in *M.*
421 *muscosa,* connected to the MBp by neurites (Steinhoff et al., 2017; Figs. 1; 4B, D, F; 6D). In *C.*
422 *salei*, it is fused with the MBp, where it forms one continuous synapsin-immunoreactive domain
423 (Strausfeld & Barth, 1993; Fig. 9B). Furthermore, the mushroom body shaft, which in *C. salei* gives
424 rise to the MBbr (Strausfeld & Barth, 1993; Fig. 9B) is absent or fused with the MBp in *M.*
425 *muscosa.* Here, the MBbr is entirely composed of few long neurites, probably originating in SC2
426 (Fig. 1).
427
428 **4.5 Functional considerations**
429 Differences in the secondary eye visual pathways of *M. muscosa* and *C. salei* might reflect the
430 differences in the visual fields and corresponding functions of their secondary eyes. Possibly the
431 most conspicuous difference between the visual systems in the brains of *M. muscosa* and *C. salei*
432 is the pathway of the PME. While the two larger secondary eyes (ALE and PLE) are connected to
433 the mushroom bodies in *M. muscosa,* the PME are not (Fig. 10). This suggests that the PME do
434 not play a role in motion detection (Duelli, 1978; Land, 1971; Zurek et al., 2010). In *C. salei,*
435 however, the PME are important movement detectors (Schmid, 1998) connected to the
436 mushroom bodies (Fig. 9; Strausfeld & Barth, 1993).
437 Another interesting difference between the two species is the presence of the L2 in *M. muscosa*
438 (Steinhoff et al., 2017). The structure of this neuropil differs from the MG and all second order
439 visual neuropils in *C. salei,* since the L2 in *M. muscosa* lacks microglomeruli (compare Figs. 2; 3;
440 5; 9; 10). Microglomeruli might ensure a retinotopic organization of neurites within the second
441 order visual neuropils. This has been hypothesized for both *C. salei* (Strausfeld & Barth, 1993)
442 and for the PLE pathway of jumping spiders (Duelli, 1980), where no lateral connections between

individual MG were found. We suggest that while the retinotopic organization is kept in the MG, it is lost in the L2. Information from movement-detecting ALE and PLE in *M. muscosa* might be integrated not only in the MB, but also in the L2, to enable faster movement decisions. Alternatively, a microglomerular organization might be the most space-saving structure for processing of variable input (Eisthen, 2002; Hildebrand & Shepherd, 1997), and although the L2 is not composed of microglomeruli, information might still be processed in parallel without lateral connections. This would also indicate that a higher number of neurites synapse in the MG than in the L2 in *M. muscosa*.

For future studies, it would be interesting to analyze the brain architecture of early-branched off salticid species, in which the PME is large and has its own field of view (e.g. *Portia*; Land, 1985a; Maddison & Hedin, 2003). Land (1985a) suggested that in jumping spiders with a small PME, such as *M. muscosa*, the fields of view of ALE and PLE have expanded to fill the space not covered by the PME. The evolutionary transformation to a smaller PME and larger ALE and PLE might have led to visual pathways that also incorporated the L2. In early-branched off jumping spiders with large PME, it could be hypothesized that the L2 might serve as a second order visual neuropil of the PME.

4.6 Conclusion

The visual pathways of the secondary eyes in the jumping spider *Marpissa muscosa* differ from those in the wandering spider *Cupiennius salei.* Our results show that differences in size and functional roles of their eyes, are associated with fundamental differences not only in structure and arrangement (Steinhoff et al., 2017), but also in connectivity of visual neuropils and thus information flow in the visual system of their brains. *C. salei* and *M. muscosa* are both cursorial hunters that attack prey based on visual cues alone (Fenk et al., 2010). We hypothesize from the data presented here that other spider groups with stronger differences in lifestyle and sensory equipment, such as stationary hunting species, will show even more pronounced differences in the structure, arrangement and connectivity of neuropils within their brains.

CONFLICT OF INTEREST STATEMENT

The authors have no conflicts of interests.

DATA AVAILABILITY STATEMENT

The data that support the findings of this study are available from the corresponding author upon reasonable request.

AUTHOR CONTRIBUTIONS

All authors had full access to all the data in the study and take responsibility for the integrity of the data and the accuracy of data analysis. Study concept and design: POMS, AS, GU. Acquisition of data: POMS. Analysis and interpretation of data: POMS, AS. Wrote the manuscript: POMS, AS. Contributed to the writing of the manuscript: GU, SH. Obtained funding: GU, SH, POMS.

LITERATURE CITED

Babu, K. S., & Barth, F. G. (1984). Neuroanatomy of the central nervous system of the wandering spider, *Cupiennius salei* (Arachnida, Araneida). *Zoomorphology*, *104*, 344–359. https://doi.org/10.1007/BF00312185

Barth, F. G., Nakagawa, T., & Eguchi, E. (1993). Vision in the ctenid spider Cupiennius salei: spectral range and absolute sensitivity. *Journal of Experimental Biology*, *79*, 63–79. https://doi.org/ghjjagsj

Barth, F.G. (2002). The central nervous system. In Friedrich G. Barth (Ed.), *A Spiders World; Senses and Behavior* (pp. 161–174). Berlin Heidelberg: Springer.

Battelle, B. A., Calman, B. G., Andrews, A. W., Grieco, F. D., Mleziva, M. B., Callaway, J. C., & Stuart, A. E. (1991). Histamine: A putative afferent neurotransmitter in *Limulus* eyes. *Journal of Comparative Neurology*, *305*(4), 527–542. https://doi.org/10.1002/cne.903050402

Battelle, B. A., Sombke, A., & Harzsch, S. (2016). Xiphosura. In A. Schmidt-Rhaesa, S. Harzsch, & G. Purschke (Eds.), *Structure and Evolution of Invertebrate Nervous Systems* (pp. 428–442). Oxford University Press.

Becherer, C., & Schmid, A. (1999). Distribution of g-aminobutyric acid-, proctolin-, *Periplaneta* hypertrehalosaemic hormone- and FMRFamide-like immunoreactivity in the visual ganglia of the spider *Cupiennius salei* Keys. *Comparative Biochemistry and Physiology Part A*, *122*, 267–275.

Cebrià, F. (2008). Organization of the nervous system in the model planarian *Schmidtea mediterranea*: An immunocytochemical study. *Neuroscience Research*, *61*(4), 375–384. https://doi.org/10.1016/j.neures.2008.04.005

Duelli, P. (1978). Movement detection in the posterolateral eyes of jumping spiders (Evarcha arcuata, Salticidae). *Journal of Comparative Physiology A*, *124*(1), 15–26. https://doi.org/10.1007/BF00656387

Duelli, P. (1980). The neuronal organization of the posterior lateral eyes of jumping spiders (Salticidae). *Zoologische Jahrbücher: Abteilung Für Anatomie Und Ontogenie Der Tiere*, *103*(1), 17–40.

Eisthen, H. L. (2002). Why are olfactory systems of different animals so similar? *Brain, Behavior and Evolution*, *59*(5–6), 273–293. https://doi.org/10.1159/000063564

Fenk, L. M., Hoinkes, T., & Schmid, A. (2010). Vision as a third sensory modality to elicit attack behavior in a nocturnal spider. *Journal of Comparative Physiology A*, *196*(12), 957–961. https://doi.org/10.1007/s00359-010-0575-8

Fenk, L. M., & Schmid, A. (2010). The orientation-dependent visual spatial cut-off frequency in a spider. *The Journal of Experimental Biology*, *213*(Pt 18), 3111–3117. https://doi.org/10.1242/jeb.041939

Foelix, R. F. (1996). *Biology of Spiders*. Oxford University Press. https://doi.org/10.2307/1535947

Groh, C., & Rössler, W. (2011). Comparison of microglomerular structures in the mushroom body calyx of neopteran insects. *Arthropod Structure and Development*, *40*(4), 358–367. https://doi.org/10.1016/j.asd.2010.12.002

Hanström, B. (1921). Über die Histologie und vergleichende Anatomie der Sehganglien und Globuli der Araneen. *Kungliga Svenska Vetenskapsakademiens Handlingar*, *61*(12), 1–39.

Harland, D. P., Li, D., & Jackson, R. R. (2012). How jumping spiders see the world. In O. F. Lazareva, T. Shimizu, & E. A. Wasserman (Eds.), *How Animals See the World: Comparative Behavior, Biology, and Evolution of Vision* (pp. 133–164). Oxford University Press. https://doi.org/10.1093/acprof:oso/9780195334654.003.0010

Harzsch, S., & Hansson, B. S. (2008). Brain architecture in the terrestrial hermit crab <i>Coenobita clypeatus (Anomura, Coenobitidae), a crustacean with a good aerial sense of smell. *BMC*

Neuroscience, *9*(1), 1–35. https://doi.org/10.1186/1471-2202-9-58

Harzsch, S., & Müller, C. H. (2007). A new look at the ventral nerve centre of *Sagitta*: implications for the phylogenetic position of Chaetognatha (arrow worms) and the evolution of the bilaterian nervous system. *Frontiers in Zoology*, *4*(1), 14.

Harzsch, S., Vilpoux, K., Blackburn, D. C., Platchetzki, D., Brown, N. L., Melzer, R., … Battelle, B. A. (2006). Evolution of arthropod visual systems: Development of the eyes and central visual pathways in the horseshoe crab *Limulus polyphemus* Linnaeus, 1758 (Chelicerata, Xiphosura). *Developmental Dynamics*, *235*(10), 2641–2655. https://doi.org/10.1002/dvdy.20866

Harzsch, S., Wildt, M., Battelle, B., & Waloszek, D. (2005). Immunohistochemical localization of neurotransmitters in the nervous system of larval *Limulus polyphemus* (Chelicerata, Xiphosura): Evidence for a conserved protocerebral architecture in Euarthropoda. *Arthropod Structure and Development*, *34*(3), 327–342. https://doi.org/10.1016/j.asd.2005.01.006

Hesse, J., & Schreiber, S. (2015). Externalization of neuronal somata as an evolutionary strategy for energy economization. *Current Biology*, *25*(8), R324–R325. https://doi.org/10.1016/j.cub.2015.02.024

Hildebrand, J. G., & Shepherd, G. M. (1997). Mechanisms of olfactory discrimination: Converging evidence for common principles across phyla. *Annual Review of Neuroscience*, *20*(1), 595–631. https://doi.org/10.1146/annurev.neuro.20.1.595

Hill, D. E. (1975). *The structure of the central nervous system of jumping spiders of the genus* Phidippus *(Araneae: Salticidae)*. M.Sc. thesis; Oregon State University.

Homann, H. (1950). Die Nebenaugen der Araneen. *Zoologische Jahrbücher : Abteilung Für Anatomie Und Ontogenie Der Tiere*, *71*, 56–144.

Homann, H. (1952). Die Nebenaugen der Araneen. Zweite Mitteilung. *Zoologische Jahrbücher : Abteilung Für Anatomie Und Ontogenie Der Tiere*, *72*, 345–364.

Jakob, E. M., Long, S. M., Harland, D. P., Jackson, R. R., Carey, A., Searles, M. E., … Rolland, J. P. (2018). Lateral eyes direct principal eyes as jumping spiders track objects. *Current Biology*, *28*(18), R1092–R1093. https://doi.org/10.1016/j.cub.2018.07.065

Klagges, B. R. E., Heimbeck, G., Godenschwege, T. A., Hofbauer, A., Pflugfelder, G. O., Reifegerste, R., … Buchner, E. (1996). Invertebrate synapsins: a single gene codes for several isoforms in *Drosophila*. *Journal of Neuroscience*, *16*, 3145–3165.

Land, M. F. (1971). Orientation by jumping spiders in the absence of visual feedback. *The Journal of Experimental Biology*, *54*(1), 119–139.

Land, M. F. (1972). Mechanisms of orientation and pattern recognition by jumping spiders (Salticidae). In R. Wehner (Ed.), *Information Processing in the Visual Systems of Anthropods* (pp. 231–247). Springer Berlin Heidelberg.

Land, M. F. (1985a). Fields of view of the eyes of primitive jumping spiders. *Journal of Experimental Biology*, *119*, 381–384.

Land, M. F. (1985b). The morphology and optics of spider eyes. In Friedrich G. Barth (Ed.), *Neurobiology of Arachnids* (pp. 53–76). Berlin: Springer. https://doi.org/10.1007/978-3-642-70348-5_4

Land, M. F., & Barth, F. G. (1992). The quality of vision in the ctenid spider *Cupiennius salei*. *Journal of Experimental Biology*, *164*, 227–242.

Lehmann, T., & Melzer, R. R. (2013). Looking like *Limulus*? - Retinula axons and visual neuropils of the median and lateral eyes of scorpions. *Frontiers in Zoology*, *10*(1), 40. https://doi.org/10.1186/1742-9994-10-40

Lehmann, T., & Melzer, R. R. (2018). Also looking like *Limulus*? - retinula axons and visual neuropils of Amblypygi (whip spiders). *Frontiers in Zoology*, *15*(1), 52. https://doi.org/10.1186/s12983-018-0293-6

Lehmann, T., Melzer, R. R., Hörnig, M. K., Michalik, P., Sombke, A., & Harzsch, S. (2016). Arachnida (excluding scorpiones). In A. Schmidt-Rhaesa, S. Harzsch, & G. Purschke (Eds.), *Structure and Evolution of Invertebrate Nervous Systems* (pp. 453–477). Oxford: Oxford University Press.

Loesel, R., Wolf, H., Kenning, M., Harzsch, S., & Sombke, A. (2013). Architectural principles and evolution of the arthropod central nervous system. In A. Minelli (Ed.), *Arthropod Biology and Evolution* (pp. 299–342). Berlin Heidelberg: Springer-Verlag. https://doi.org/10.1007/978-3-642-36160-9

Long, S. M. (2016). *Spider Brain Morphology & Behavior*. PhD thesis; University of Massachusetts,

Amherst.

Maddison, W. P., & Hedin, M. C. (2003). Jumping spider phylogeny (Araneae: Salticidae). *Invertebrate Systematics*, *17*(4), 529. https://doi.org/10.1071/is02044

Morehouse, N. I., Buschbeck, E. K., Zurek, D. B., Steck, M., & Porter, M. L. (2017). Molecular evolution of spider vision: New opportunities, familiar players. *Biological Bulletin*, *233*(1), 21–38. https://doi.org/10.1086/693977

Nagata, T., Arikawa, K., & Kinoshita, M. (2019). Photoreceptor projection from a four-tiered retina to four distinct regions of the first optic ganglion in a jumping spider. *Journal of Comparative Neurology*, pp. 1–14. https://doi.org/10.1002/cne.24584

Nässel, D. R. (1999). Histamine in the brain of insects: a review. *Microscopy Research and Technique*, *44*(2–3), 121–136. https://doi.org/10.1002/(SICI)1097-0029(19990115/01)44:2/3<121::AID-JEMT6>3.0.CO;2-F

Orlando, E., & Schmid, A. (2011). Colour blindness of the movement-detecting system of the spider *Cupiennius salei*. *Journal of Experimental Biology*, *214*(4), 546–550. https://doi.org/10.1242/jeb.051672

Ott, S. R. (2008). Confocal microscopy in large insect brains: Zinc-formaldehyde fixation improves synapsin immunostaining and preservation of morphology in whole-mounts. *Journal of Neuroscience Methods*, *172*(2), 220–230. https://doi.org/10.1016/j.jneumeth.2008.04.031

Richter, S., Loesel, R., Purschke, G., Schmidt-Rhaesa, A., Scholtz, G., Stach, T., … Harzsch, S. (2010). Invertebrate neurophylogeny: suggested terms and definitions for a neuroanatomical glossary. *Frontiers in Zoology*, *7*, 29. https://doi.org/10.1186/1742-9994-7-29

Rössler, W., Spaethe, J., & Groh, C. (2017). Pitfalls of using confocal- microscopy based automated quantification of synaptic complexes in honeybee mushroom bodies (response to Peng and Yang 2016). *Scientific Reports*, *7*, 1–5. https://doi.org/10.1038/s41598-017-11858-x

Saint Rémy, G. (1887). Contribution à l'étude du cerveau chez les Arthropodes trachéates. *Archives de Zoologie Experimentale et Générale*.

Schmid, A. (1998). Different functions of different eye types in the spider Cupiennius salei. *The Journal of Experimental Biology*, *201*, 221–225.

Schmid, A., & Duncker, M. (1993). Histamine immunoreactivity in the central nervous system of

the spider Cupiennius salei. *Cell & Tissue Research*, *273*(3), 533–545. https://doi.org/10.1007/BF00333707

Schulze, E., & Graupner, H. (1960). *Anleitung zum mikroskopisch-technischen Arbeiten in Biologie und Medizin*. Akademische Verlagsgesellschaft.

Sombke, A., & Harzsch, S. (2015). Immunolocalization of histamine in the optic neuropils of *Scutigera coleoptrata* (Myriapoda: Chilopoda) reveals the basal organization of visual systems in Mandibulata. *Neuroscience Letters*, *594*, 111–116. https://doi.org/10.1016/j.neulet.2015.03.029

Sombke, A., Harzsch, S., & Hansson, B. S. (2011). Organization of deutocerebral neuropils and olfactory behavior in the centipede *Scutigera coleoptrata* (Linnaeus, 1758) (Myriapoda: Chilopoda). *Chemical Senses*, *36*(1), 43–61. https://doi.org/10.1093/chemse/bjq096

Sombke, A., Lipke, E., Michalik, P., Uhl, G., & Harzsch, S. (2015). Potential and limitations of x-ray micro-computed tomography in arthropod neuroanatomy: a methodological and comparative survey. *Journal of Comparative Neurology*, *523*(8), 1281–1295. https://doi.org/10.1002/cne.23741

Spano, L., Long, S. M., & Jakob, E. M. (2012). Secondary eyes mediate the response to looming objects in jumping spiders (Phidippus audax, Salticidae). *Biology Letters*, *8*(6), 949–951. https://doi.org/10.1098/rsbl.2012.0716

Steinhoff, P. O. M., Liedtke, J., Sombke, A., Schneider, J. M., & Uhl, G. (2018). Early environmental conditions affect the volume of higher-order brain centers in a jumping spider. *Journal of Zoology*, *304*(3), 182–192. https://doi.org/10.1111/jzo.12512

Steinhoff, P. O. M., Sombke, A., Liedtke, J., Schneider, J. M., Harzsch, S., & Uhl, G. (2017). The synganglion of the jumping spider *Marpissa muscosa* (Arachnida: Salticidae): Insights from histology, immunohistochemistry and microCT analysis. *Arthropod Structure and Development*, *46*(2), 156–170. https://doi.org/10.1016/j.asd.2016.11.003

Strausfeld, N. J., & Barth, F. G. (1993). Two visual systems in one brain: Neuropils serving the secondary eyes of the spider Cupiennius salei. *The Journal of Comparative Neurology*, *328*(1), 43–62. https://doi.org/10.1002/cne.903280105

Strausfeld, N. J., Weltzien, P., & Barth, F. G. (1993). Two visual systems in one brain: Neuropils

serving the principal eyes of the spider *Cupiennius salei*. *The Journal of Comparative Neurology*, *328*(1), 63–75. https://doi.org/10.1002/cne.903280105

Sullivan, J. M., Benton, J. L., Sandeman, D. C., & Beltz, B. S. (2007). Adult neurogenesis: A common strategy across diverse species. *Journal of Comparative Neurology*, *500*(3), 574–584. https://doi.org/10.1002/cne.21187

Weltzien, P., & Barth, F. G. (1991). Volumetric measurements do not demonstrate that the spider brain "central body" has a special role in web building. *Journal of Morphology*, *208*(1), 91–98. https://doi.org/10.1002/jmor.1052080104

Yamashita, S., & Tateda, H. (1976). Spectral sensitivities of jumping spider eyes. *Journal of Comparative Physiology A*, *105*(1), 29–41. https://doi.org/10.1007/BF01380051

Yamashita, S., & Tateda, H. (1978). Spectral sensitivities of the anterior median eyes of the orb web spiders, *Argiope bruennichii* and *A. amoena*. *Journal of Experimental Biology*, *74*(1), 47–57.

Zurek, D. B., & Nelson, X. J. (2012a). Hyperacute motion detection by the lateral eyes of jumping spiders. *Vision Research*, *66*, 26–30. https://doi.org/10.1016/j.visres.2012.06.011

Zurek, D. B., & Nelson, X. J. (2012b). Saccadic tracking of targets mediated by the anterior-lateral eyes of jumping spiders. *Journal of Comparative Physiology A*, *198*(6), 411–417. https://doi.org/10.1007/s00359-012-0719-0

Zurek, D. B., Taylor, A. J., Evans, C. S., & Nelson, X. J. (2010). The role of the anterior lateral eyes in the vision-based behaviour of jumping spiders. *The Journal of Experimental Biology*, *213*, 2372–2378. https://doi.org/10.1242/jeb.042382

Tables

Table 1 Primary and secondary antibodies

Labeling reagent	Dilution and specifications
Primary	
Monoclonal anti-synapsin antibody produced in mouse (AB_528479)	1:1000, DSHB 3C11 Steinhoff et al. (2017), this study
Polyclonal anti-acetylated α-tubulin antibody produced in rabbit (AB_2637882)	1:1000, ThermoFisher PA5-58711
Monoclonal anti-acetylated α-tubulin antibody produced in mouse (AB_477585)	1:1000, Sigma Aldrich T6793
Monoclonal anti-histamine antibody produced in rabbit (AB_1541510)	1:1000, Progen 16043 Harzsch et al. (2005), Sombke and Harzsch 2015
Secondary	
Polyclonal Cy3 anti-mouse IgG secondary anti- body produced in goat (AB_2338680)	1:500, Jackson Immuno Research, 115–165-003
Polyclonal Alexa 488 anti-rabbit IgG secondary antibody produced in goat (AB_2534074)	1:500, Invitrogen, A11006
Alexa Fluor 488 phalloidin (AB_2315147)	1:50, Molecular Probes A-12379
Hoechst 33258	1:1000, Sigma 14530
YOYO 1 491	Molecular Probes Y-3601

Table 2 Methods and antisera combinations

Methods	Antisera combinations/ staining	Coupled with	Specimens
Wholemount	anti-synapsin	Cy3 anti-mouse (goat)	5
Vibratome sections (80 µm)	anti-synapsin (mouse) anti-acetylated-α-tubulin (rabbit)	Cy3 anti-mouse (goat) Alexa Fluor 488 anti-rabbit (goat) Nuclear labeling: Hoechst 33258	10
	anti-acetylated-α-tubulin (mouse)	Nuclear labeling: YOYO	6
	anti-histamine (rabbit)	Alexa Fluor 488 anti-rabbit (goat)	4
	anti-synapsin (mouse)	Cy3 anti-mouse (goat) Phalloidin	5
Paraffin sections (5 µm)	Azan-novum	/	2
microCT scans	1% idodine (in 99% ethanol)	/	4

688 **Figures and supporting information**

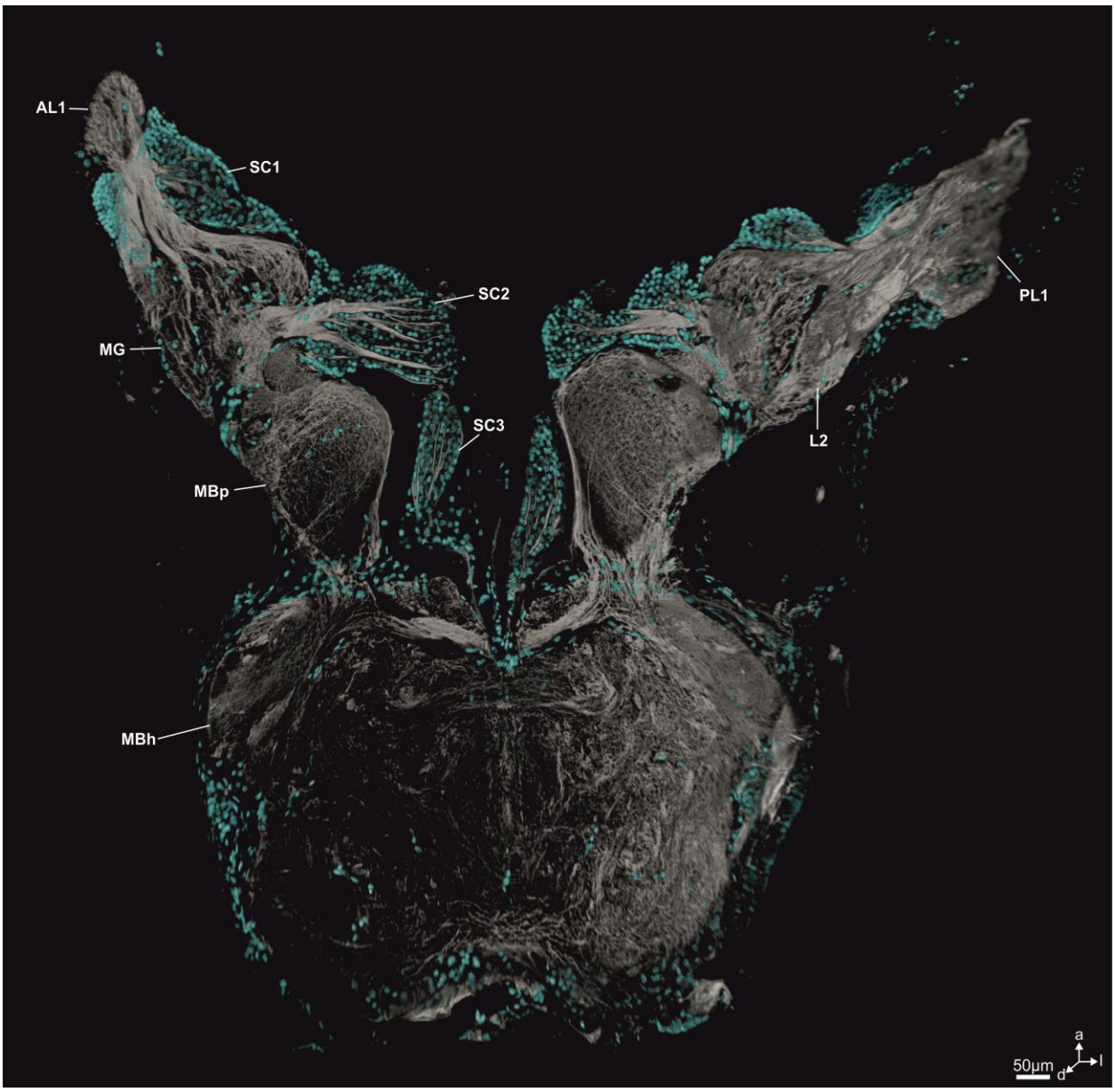

689

690 **Figure 1.** Maximum projection of an image stack (clsm), showing tubulin-immunoreactivity (grey)
691 and somata (blue) in the protocerebrum of *Marpissa muscosa*. The AL1 and PL1 are connected
692 to both, the MG and the L2. The neurites forming these connections originate in SC1. The MG
693 and the L2 are connected to the MBp via neurites, which originate in the SC2. The two MBp are
694 connected with each other via the mushroom body bridge, which is formed by long neurites that
695 project along the periphery of the MBp and seem to originate in the SC2. Some of these long
696 neurites also connect the MBp with the MBh. Other neurites originate in SC3 and enter the

protocerebrum medially. **Abbreviations: a** anterior, **AL1** first order visual neuropil of the anterior lateral eyes, **d** dorsal, **l** lateral, **L2** shared second order visual neuropil of the anterior lateral and posterior lateral eyes, **MBh** mushroom body haft, **MBp** mushroom body pedunculus, **MG** array of microglomeruli, **SC1-3** soma cluster 1-3.

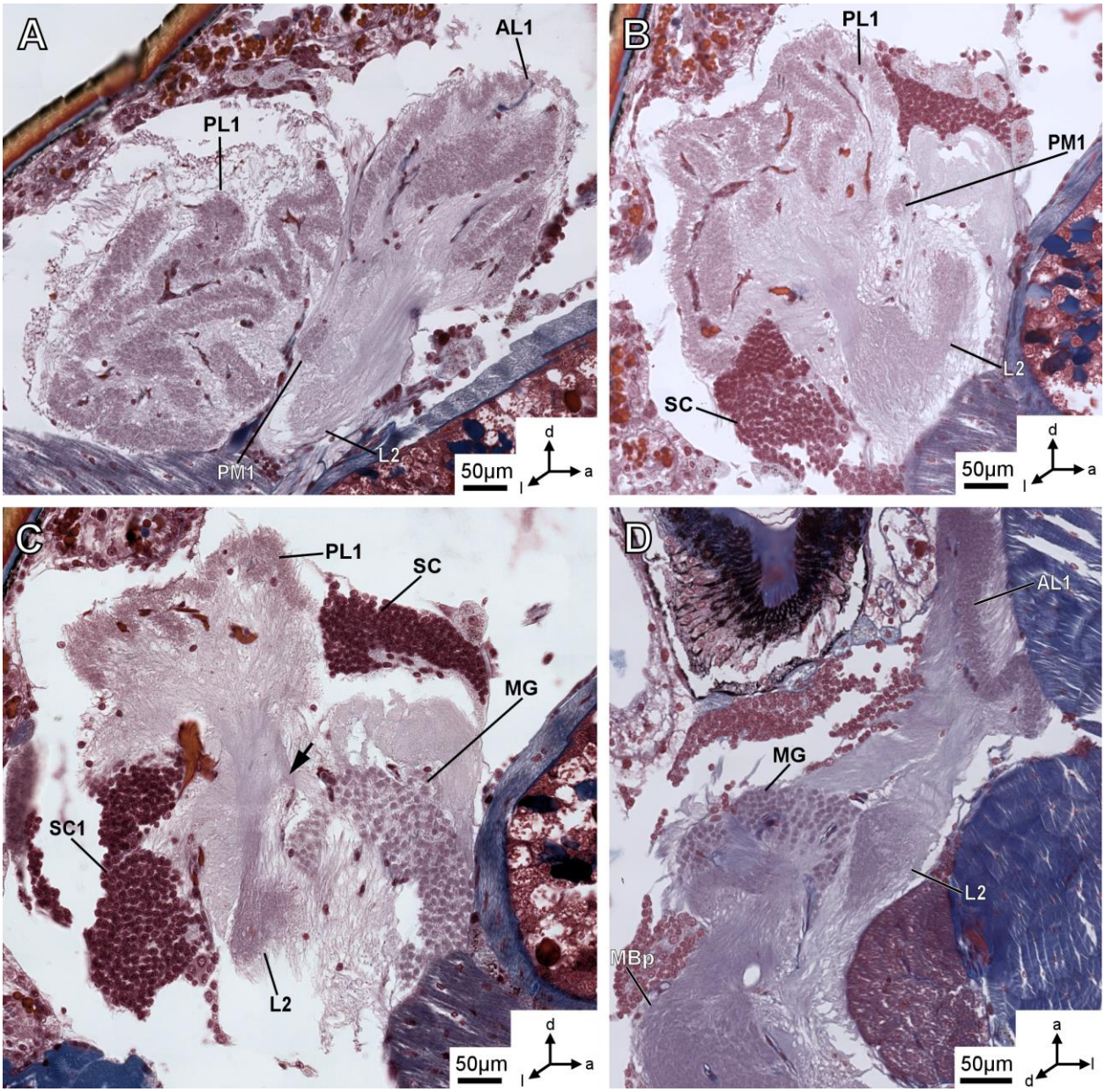

Figure 2. Paraffin sections through the anterior protocerebrum of *Marpissa muscosa.* **A** Sagittal section showing the convoluted surface and columnar structure of the AL1 and PL1. The optic nerve of the PME passes through between AL1 and PL1 and terminates in the PM1. The connection between AL1 and L2 is visible. **B** Sagittal section showing how the PL1 connects to the posterior lobe of the L2. **C** Sagittal section showing several neurites that connect the PL1 with the MG (highlighted by arrow), as well as some of the neurites connecting the PL1 with the L2. **D** Horizontal section, showing the connection of the AL1 with both, the MG and the L2. **Abbreviations: a** anterior, **AL1** first order visual neuropil of the anterior lateral eyes, **d** dorsal, **l**

lateral, **L2** shared second order visual neuropil of the anterior lateral and posterior lateral eyes, **MBp** mushroom body pedunculus, **MG** array of microglomeruli, **PL1** first order visual neuropil of the posterior lateral eyes, **PM1** first order visual neuropil of the posterior median eyes, **SC** soma cluster.

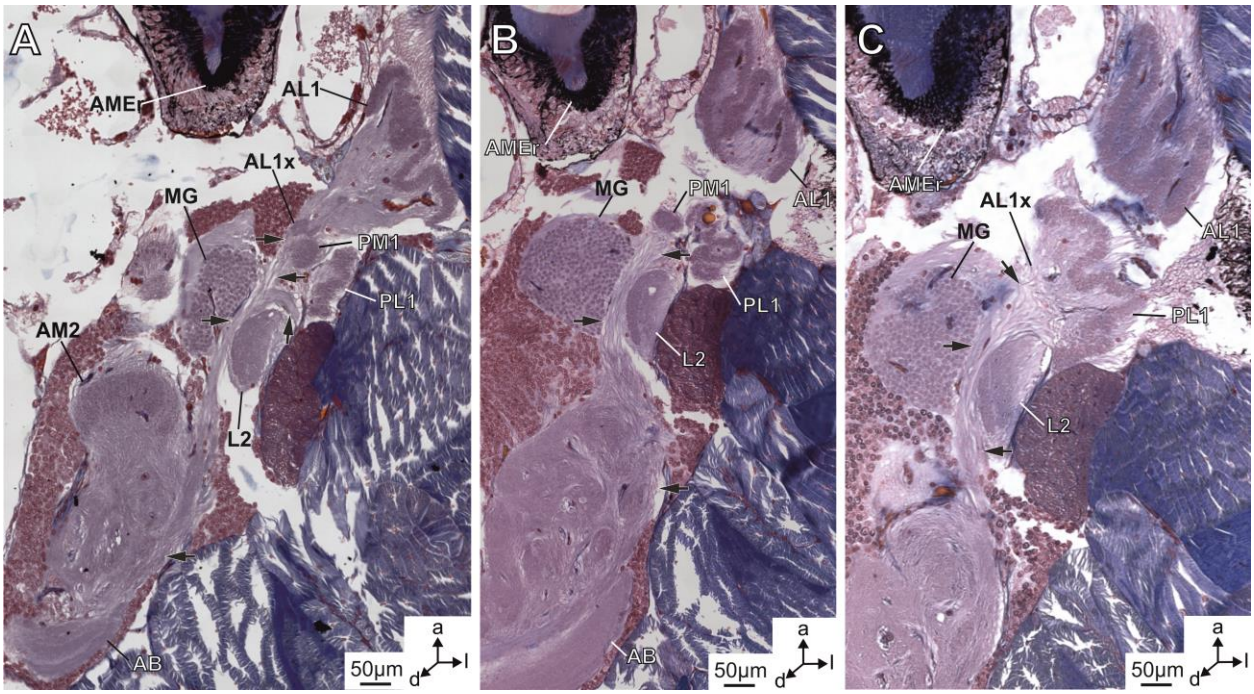

764

765 **Figure 3.** Horizontal paraffin sections through the protocerebrum of *Marpissa muscosa.* **A**
766 Neurites that connect the AL1 with the AB probably synapse in the AL1x. Long neurites
767 connecting the PL1 with the AB are visible curving around L2. Other long neurites contributing to
768 the tract to the AB synapse in PM1. Arrows point to neurites contributing to the tract between
769 first order visual neuropils of the secondary eyes and the arcuate body. **B** In a more ventral
770 section, more parallel-arranged neurites can be differentiated that connect the PM1 with the AB.
771 **C** Neurites that connect the PL1 with the AB probably synapse in the PL1x. **Abbreviations: a**
772 anterior, **AB** arcuate body, **AL1** first order visual neuropil of the anterior lateral eyes, **AL1x**
773 neuropilar subunit of the AL1, **AM2** second order visual neuropil of the anterior median eyes,
774 **AMEr** retina of the anterior median eyes, **d** dorsal, **l** lateral, **L2** shared second order visual
775 neuropil of the anterior lateral and posterior lateral eyes, **MBp** mushroom body pedunculus, **MG**
776 array of microglomeruli, **PL1** first order visual neuropil of the posterior lateral eyes, **PL1x**
777 neuropilar subunit of the PL1, **PM1** first order visual neuropil of the posterior median eyes.

778

779

780

781

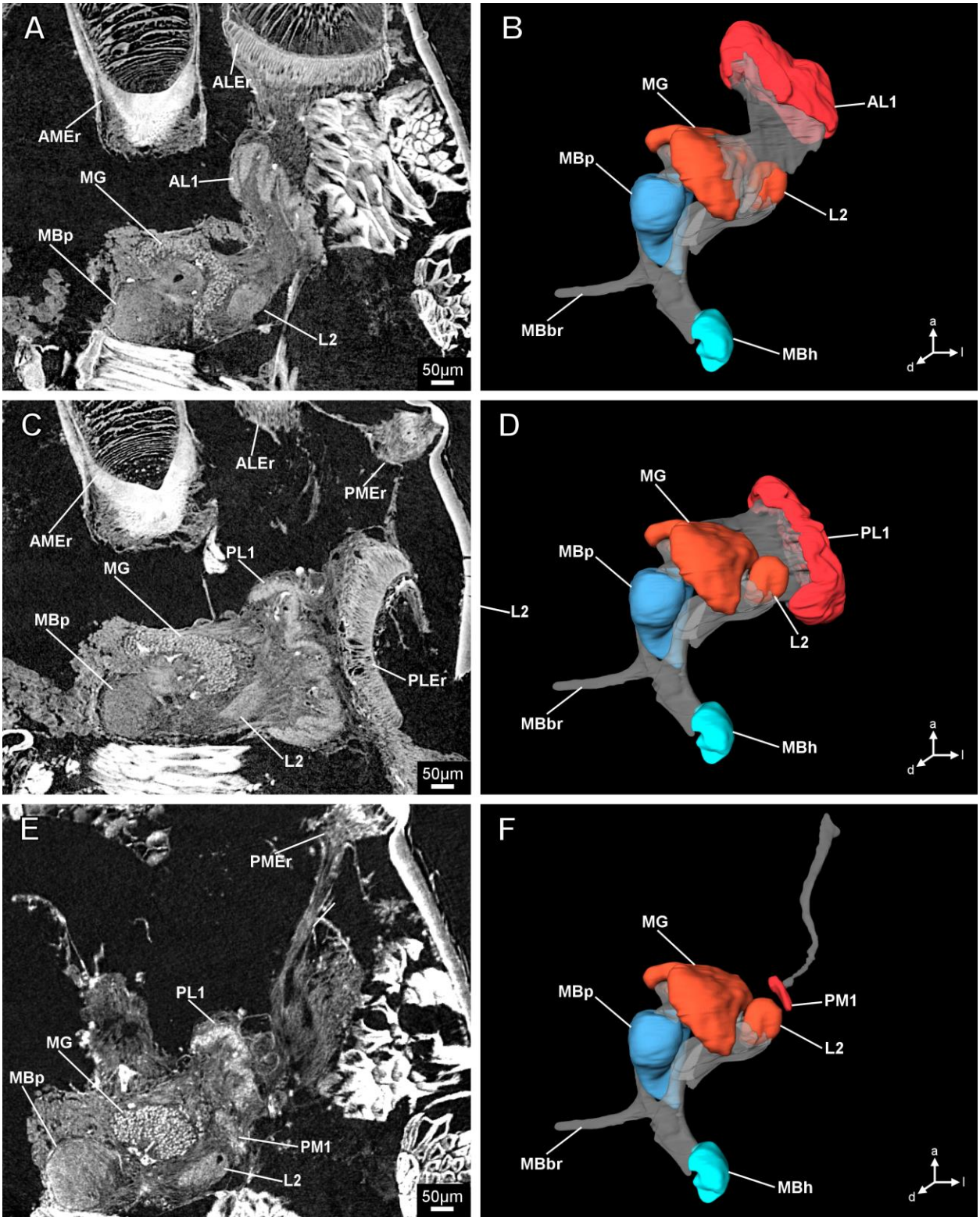

Figure 4. Protocerebral neuropils depicted in different virtual horizontal sections obtained by microCT analysis (**A, C, E**) and three-dimensional reconstructions based on microCT image stacks (**B, D, F**). **A** + **B** The retina of the ALE is located very closely to its first order visual neuropil, the

AL1. The AL1 has a convoluted surface and is connected to the MG and the L2. **C** + **D** The retina of the PLE almost comes in contact with its first order visual neuropil, the PL1. The PL1 has a convoluted surface and is connected to the MB and the L2. **E** + **F** A comparatively long optic nerve connects the retina of the PME with its first order visual neuropil, the PM1. See supporting information for an interactive 3D-visualization of the microCT reconstruction. **Abbreviations: a** anterior, **AL1** first order visual neuropil of the anterior lateral eyes, **ALEr** retina of the anterior lateral eyes, **AMEr** retina of the anterior median eyes, **d** dorsal, **l** lateral, **L2** shared second order visual neuropil of the anterior lateral and posterior lateral eyes, **MBbr** mushroom body bridge, **MBh** mushroom body haft, **MBp** mushroom body pedunculus, **MG** array of microglomeruli, **PL1** first order visual neuropil of the posterior lateral eyes, **PLEr** retina of the posterior lateral eyes, **PM1** first order visual neuropil of the posterior median eyes, **PMEr** retina of the posterior median eyes.

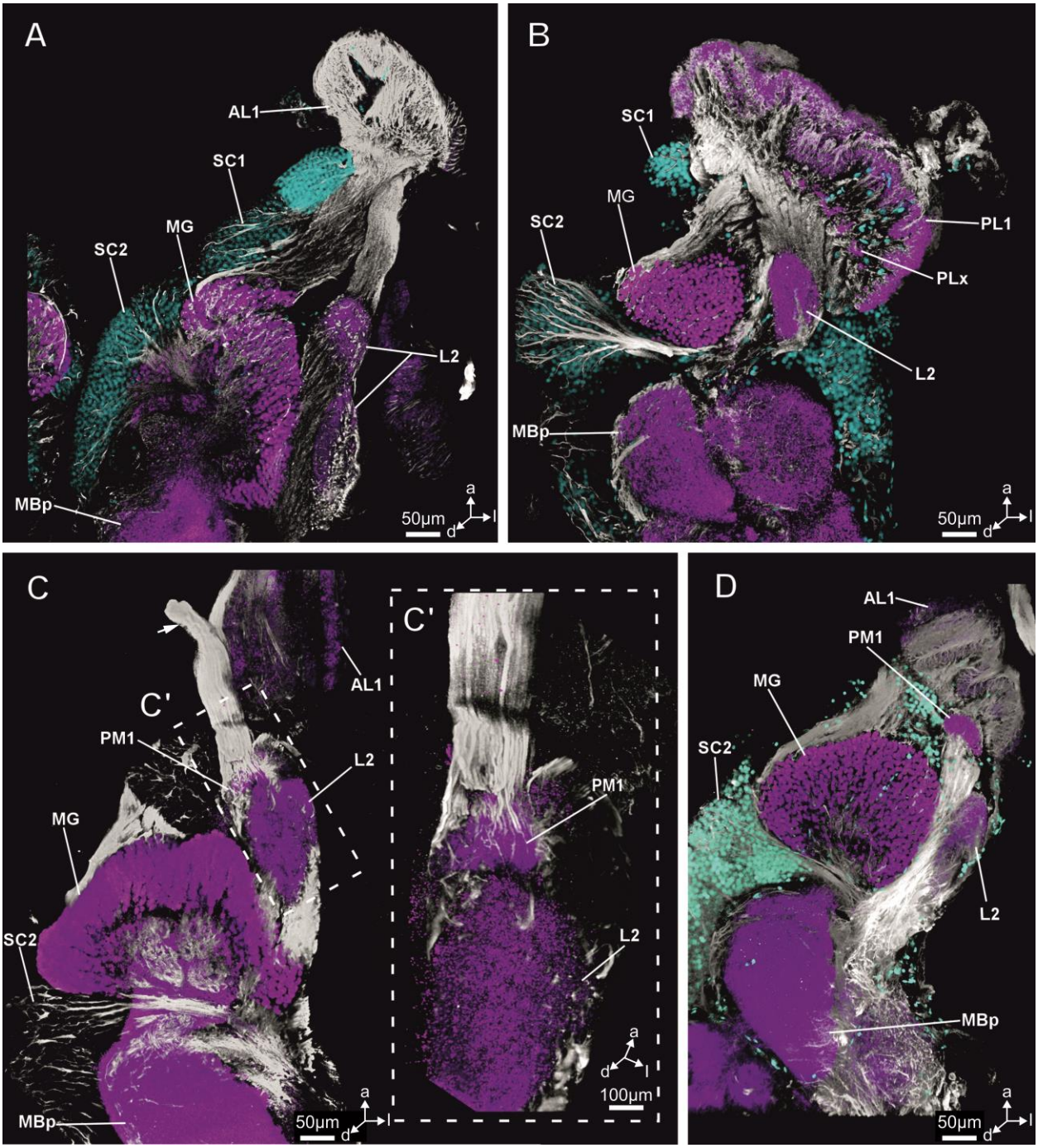

Figure 5. Maximum projections of image stacks (clsm) showing tubulin-immunoreactivity (grey), synapsin-immunoreactivity (magenta) and somata (blue) in the secondary eye visual pathway of *Marpissa muscosa*. **A** The AL1 is connected to the MG and the L2 via two prominent neurite tracts. Some of the neurites contributing to these tracts originate in SC1. Neurites connecting the MG with the MBp originate in SC2. **B** The PL1 is connected to the MG and the L2 via two

821 prominent neurite tracts. Some neurites that arise in SC2 pass between MG and MBp towards
822 the L2. **C** The optic nerve of the PME (highlighted by arrow) terminates in the PM1. **C'** Higher
823 magnification of C, showing the termination site of the PME optic nerve in the PM1. **D** Neurites
824 from the PM1 pass between MG and L2. **Abbreviations: a** anterior, **AL1** first order visual neuropil
825 of the anterior lateral eyes, **d** dorsal, **l** lateral, **L2** shared second order visual neuropil of the
826 anterior lateral and posterior lateral eyes, **MBp** mushroom body pedunculus, **MG** array of
827 microglomeruli, **PL1** first order visual neuropil of the posterior lateral eyes, **PL1x** neuropilar
828 subunit of the PL1, **PM1** first order visual neuropil of the posterior median eyes, **SC1-2** soma
829 cluster 1-2.
830
831
832
833
834
835
836
837
838
839
840
841
842
843
844
845
846
847
848
849

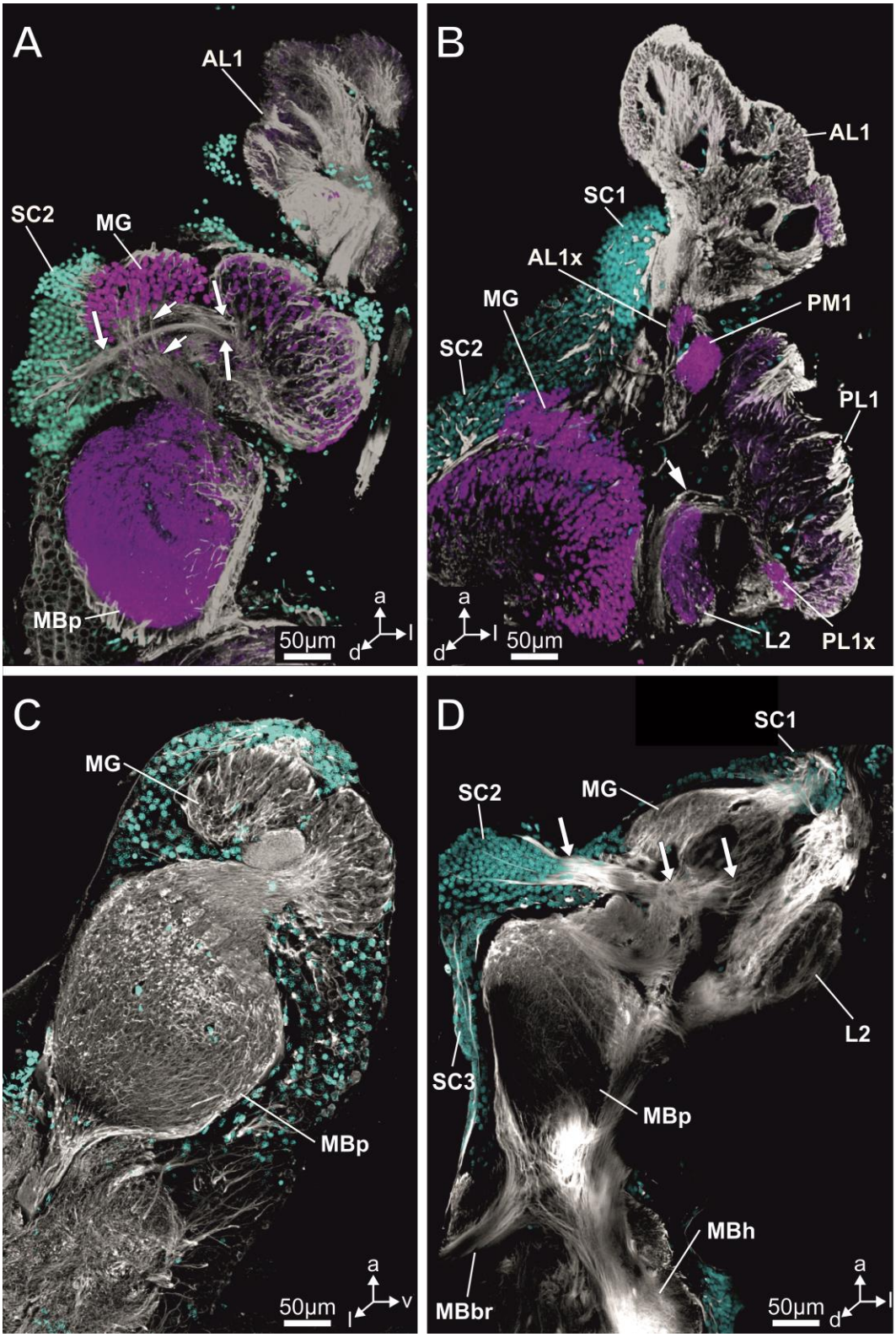

850

851 **Figure 6.** Maximum projections of image stacks (clsm) showing tubulin-immunoreactivity (grey),

852 synapsin-immunoreactivity (magenta) and somata (blue) in the secondary eye visual pathway of

853 *Marpissa muscosa*. **A** Horizontal section through AL1, MBp and MG. The AL1 connects to one of
854 the two tightly adjoining clusters of MG. Arrows point to 'stem neurites' connecting SC2 and MG.
855 Arrowheads point to neurites connecting the MG with the MBp. **B** Horizontal section through
856 visual neuropils. The PM1 is situated between AL1 and PL1, MG appear as a uniform array. The
857 arrowhead points to neurites connecting PL1 with AB, neurites probably synapse in the PL1x. **C** A
858 sagittal section through MG and MBp reveals two distinct clusters of MG and the chiasm formed
859 by neurites that connect MG with MBp. **D** Tubulin-immunoreactivity shows long peripheral
860 neurites contributing to the MBbr and connecting the MBp with the MBh. Arrows point to 'stem
861 neurites' connecting SC2 with the MG. **Abbreviations: a** anterior, **AL1** first order visual neuropil
862 of the anterior lateral eyes, **AL1x** neuropilar subunit of the AL1, **d** dorsal, **l** lateral, **L2** shared
863 second order visual neuropil of the anterior lateral and posterior lateral eyes, **MBbr** mushroom
864 body bridge, **MBh** mushroom body haft, **MBp** mushroom body pedunculus, **MG** array of
865 microglomeruli, **PL1** first order visual neuropil of the posterior lateral eyes, **PL1x** neuropilar
866 subunit of the PL1, **PM1** first order visual neuropil of the posterior median eyes, **SC1-3** soma
867 cluster 1-3.
868
869
870
871
872
873
874
875
876
877
878
879
880
881

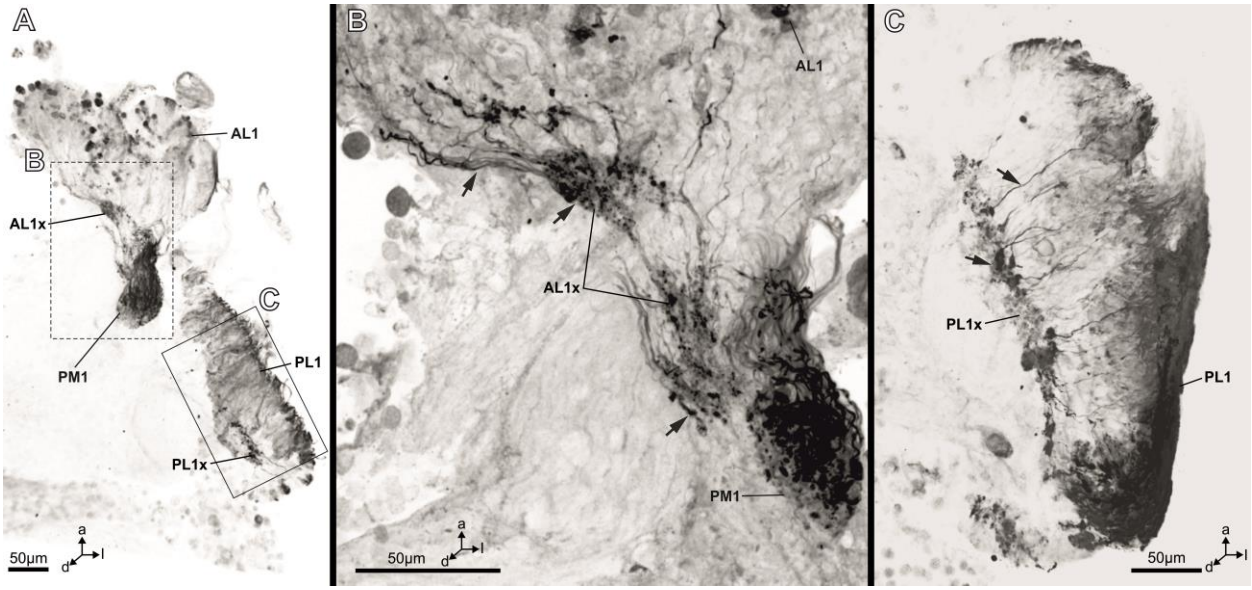

Figure 7. Maximum projections of image stacks (clsm), showing histamine-immunoreactivity in horizontal sections through the anteriormost protocerebrum of *Marpissa muscosa*. **A** Overview, shows strong histamine-immunoreactivity of retinula cell axon terminals in the AL1 and its substructure the AL1x, as well as in the PL1 and its substructure the PL1x. Retinula cell axons of the PME and their terminals in the PM1 exhibit strong histamine-immunoreactivity. **B** Magnification showing histamine-immunoreactive retinula cell axons and their terminals in the AL1x and PM1. Note the close spatial association of AL1x and PM1; AL1x is somewhat distorted due to sectioning. Arrows point to histamine-immunoreactive retinula cell axons and their terminals. **C** Magnification showing histamine-immunoreactive retinula cell axons and their terminals in the PL1 and PL1x. Arrows point to a retinula cell axon and a large terminal in the PL1x. **Abbreviations: a** anterior, **AL1** first order visual neuropil of the anterior lateral eyes, **AL1x** neuropilar subunit of the AL1, **d** dorsal, **l** lateral, **PL1** first order visual neuropil of the posterior lateral eyes, **PL1x** neuropilar subunit of the PL1, **PM1** first order visual neuropil of the posterior median eyes.

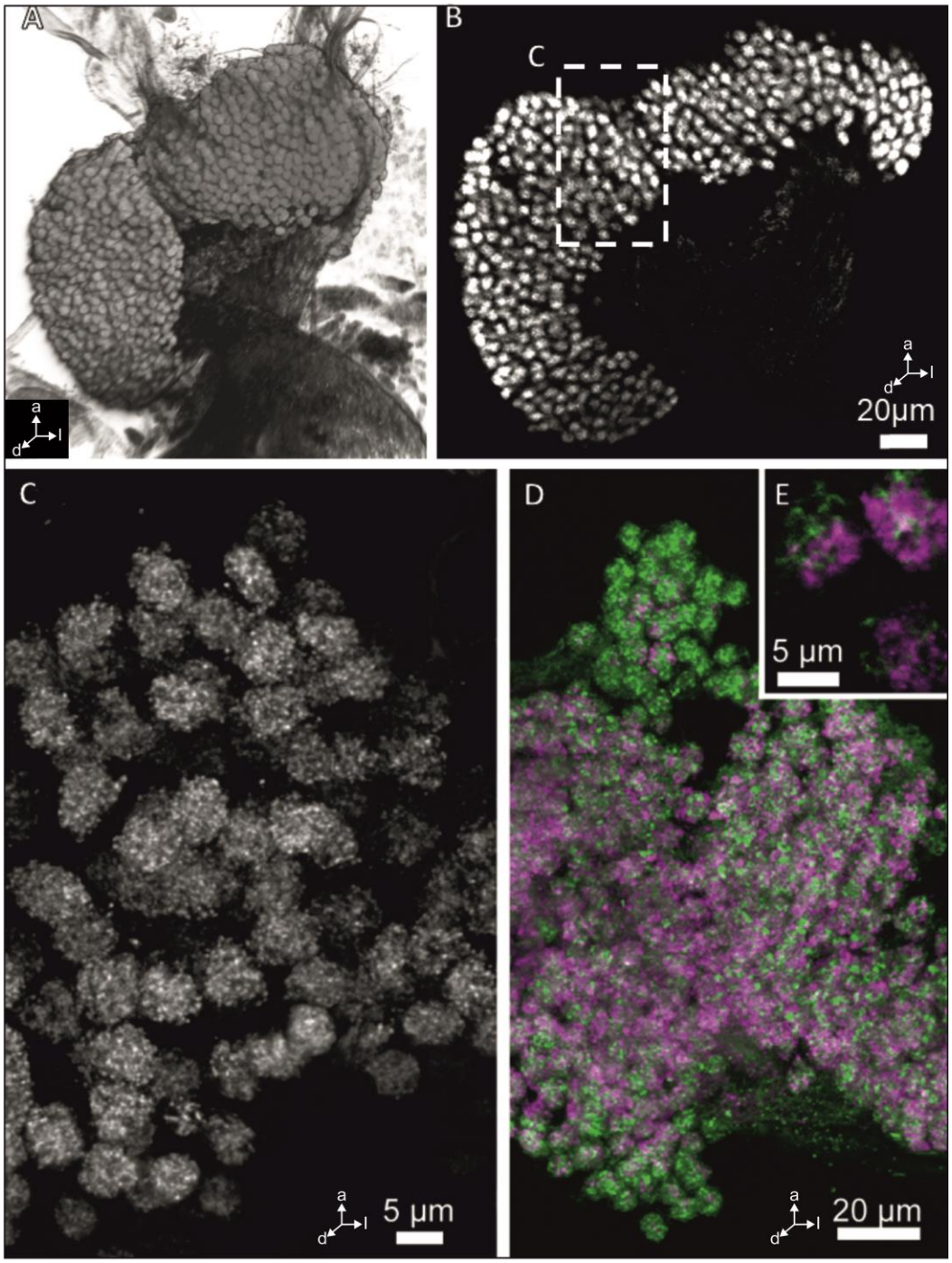

Figure 8. The array of microglomeruli in the secondary eye visual pathway of *Marpissa muscosa.* **A** Three-dimensional volume rendering of an anti-synapsin labeled whole-mount, view from posterodorsal. Note the two distinct clusters of microglomeruli that adjoin closely and coat the MBp anteriorly. **B** Single optical section of the MG within an anti-synapsin labeled whole-mount shows two distinct clusters of MG and a chiasm of neurites connecting them to the MBp. **C** Stack

of optical sections through the MG (maximum intensity projection), showing synapsin-immunoreactivity. The glomerular subunits within each individual MG may represent synaptic boutons. **D** Anti-synapsin (magenta) and phalloidin (green) double–labeling reveals glomerular substructures (boutons) of the MG. **E** Three individual MG with glomerular substructures (boutons) labeled by anti-synapsin and phalloidin.

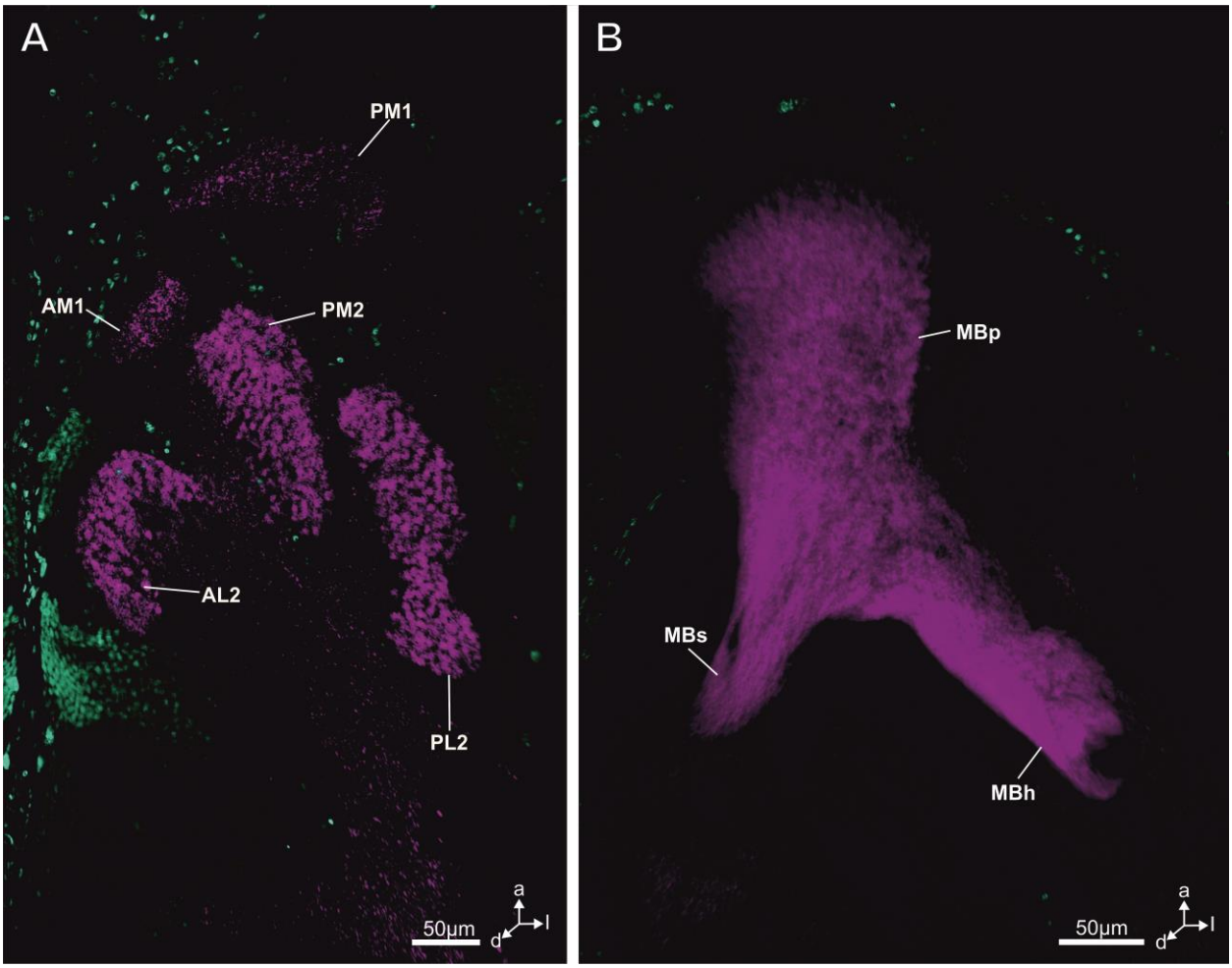

Figure 9. Maximum projection of an image stack (clsm) showing synapsin-immunoreactivity (magenta) and somata (cyan) in the secondary eye visual system of *Cupiennius salei*. **A** Every eye is associated with its own second order visual neuropil; AL2, PM2, and PL2. All three second order visual neuropils are sub-structured into microglomeruli similar to those found in the MG in *Marpissa muscosa.* **B** The MB of *C. salei* consists of a MBp, MBh and MBs. All three substructures form a continuous synapsin-rich neuropil. **Abbreviations: a** anterior, **AL2** second order visual neuropil of the anterior lateral eyes, **AM1** first order visual neuropil of the anterior median eyes, **d** dorsal, **l** lateral, **MBh** mushroom body haft, **MBp** mushroom body pedunculus, **MBs** mushroom body shaft, **PL2** second order visual neuropil of the posterior lateral eyes, **PM1** first order visual neuropil of the posterior median eyes, **PM2** second order visual neuropil of the posterior median eyes.

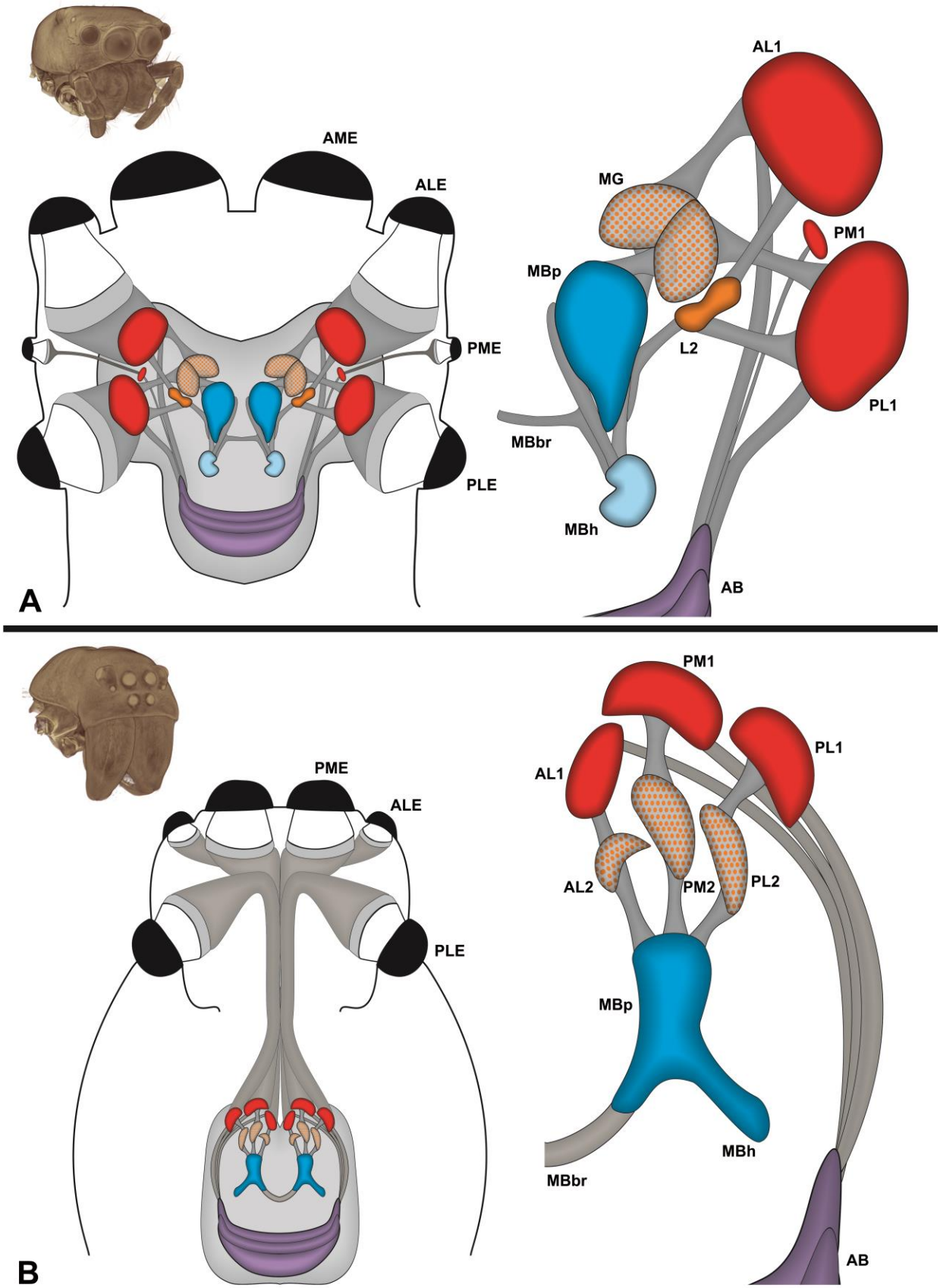
AME
ALE
PME
PLE
AL1
MG
PM1
MBp
L2
PL1
MBbr
MBh
AB
A
PM1
PL1
AL1
PME
ALE
AL2
PM2
PL2
PLE
MBp
MBh
MBbr
AB
B

950

Figure 10. Schematic representations of the secondary eye visual pathways in the brains of **A** *Marpissa muscosa* and **B** *Cupiennius salei.* Insets top left: 3D volume rendering of the prosomata of **A** *M. muscosa* and **B** *C. salei*, based on microCT analysis. **B** Anterior median eyes concealed by posterior median eyes. **Abbreviations: AB** arcuate body, **AL1** first order visual neuropil of the anterior lateral eyes, **AL2** second order visual neuropil of the anterior lateral eyes, **ALE** anterior lateral eye, **AME** anterior median eye, **L2** shared second order visual neuropil of the anterior lateral and posterior lateral eyes, **MBbr** mushroom body bridge, **MBh** mushroom body haft, **MBp** mushroom body pedunculus, **MG** array of microglomeruli, **PL1** first order visual neuropil of the posterior lateral eyes, **PL2** second order visual neuropil of the posterior lateral eyes, **PLE** posterior lateral eye, **PME** posterior median eye, **PM1** first order visual neuropil of the posterior median eyes, **PM2** second order visual neuropil of the posterior median eyes.

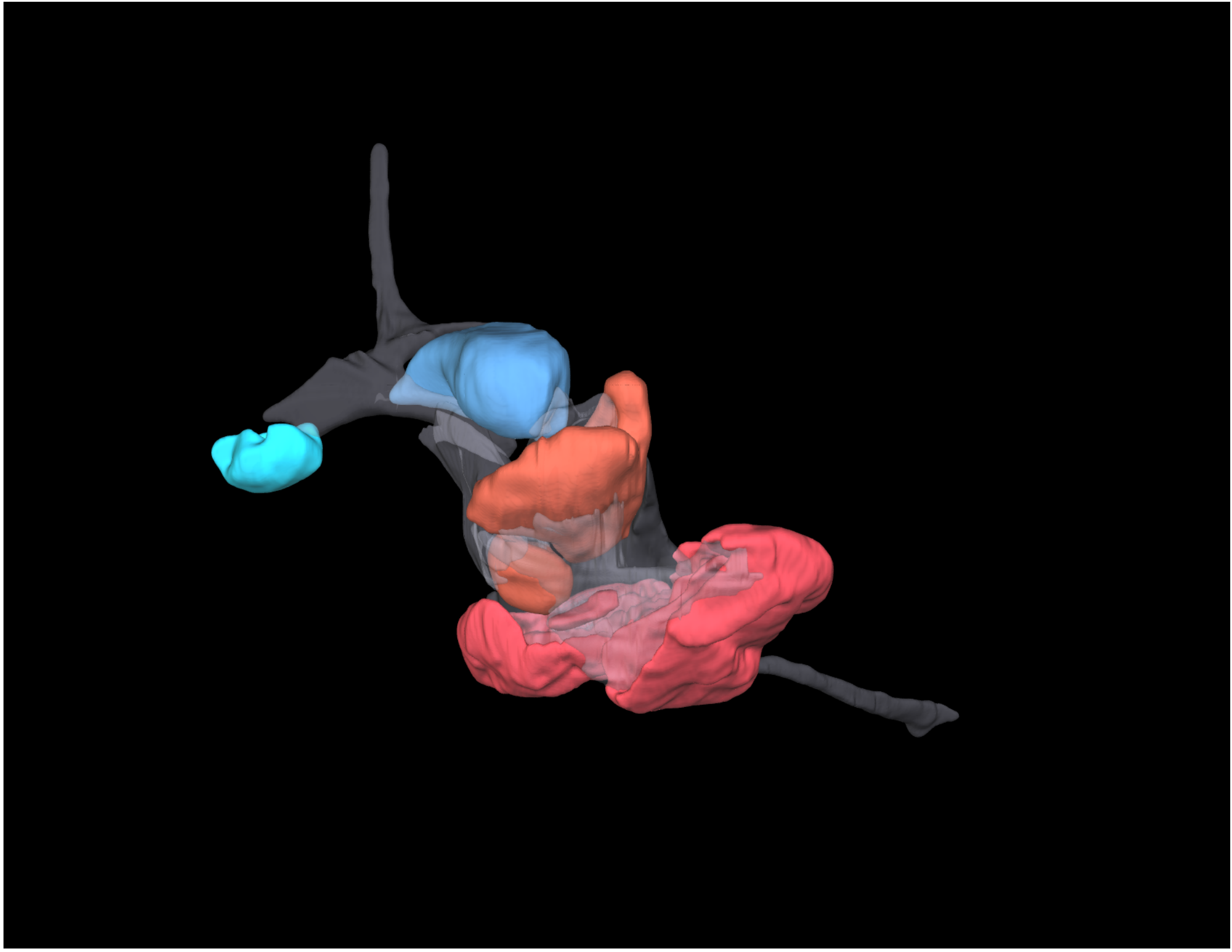

Figure S1: Interactive 3D visualization of protocerebral neuropils based on reconstruction of microCT image stacks. The AL1 and the PL1 both are connected to the MG and the L2. A comparatively long optic nerve connects the retina of the PME with its first order visual neuropil, the PM1. **Abbreviations: AL1** first order visual neuropil of the anterior lateral eyes, **L2** shared second order visual neuropil of the anterior lateral and posterior lateral eyes, **MBbr** mushroom body bridge, **MBh** mushroom body haft, **MBp** mushroom body pedunculus, **MG** array of microglomeruli, **PL1** first order visual neuropil of the posterior lateral eyes, **PM1** first order visual neuropil of the posterior median eyes.